Ocean Engineering 262 (2022) 112241

Contents lists available at ScienceDirect

Ocean Engineering

journal homepage: www.elsevier.com/locate/oceaneng

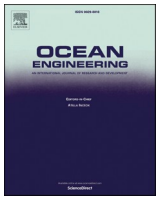

Numerical and experimental study on the influence of a moonpool on motion performance and stability of a drillship

Zhen Liu [a], Jinhui He [a], Yang Meng [a], Haibin Zhang [a], Yaohua Zhou [b], Longbin Tao [c,*]

[a] Marine Design and Research Institute of China, Shanghai Key Laboratory of Ship Engineering, Shanghai, 200011, China
[b] Shanghai Rules & Research Institute, China Classification Society, Shanghai, 200135, China
[c] Department of Naval Architecture, Ocean and Marine Engineering, University of Strathclyde, Glasgow, G4 0LZ, United Kingdom

ARTICLE INFO

Keywords:
Drillship
Moonpool
Motion performance
Stability

ABSTRACT

The existence of a moonpool may affect motion characteristics and stability of a drillship. This paper presents numerical and experimental study on the influence of the configuration of a moonpool on the motion performance and stability of a drillship under the condition of a constant displacement. Ship hydrostatics and three-dimensional (3D) potential flow theory are employed to calculate the static stability curves (GZ curves) and motion response amplitude operators (RAOs) of the drillship with conjoined double moonpools, separated double moonpools and single rectangular moonpools, respectively. Numerical model is validated by sea-keeping model tests of the drillship with a conjoined double moonpool carried out in towing tank. It is found that there is a critical heeling angle for the static stability curve of the drillship. The variation of the opening size of the moonpool is found to merely have significant effect on the heave RAOs of the drillship near the piston mode resonance period, while slightly influence on the pitch RAOs near the sloshing mode resonance period. It is demonstrated that smaller or larger openings of the moonpool under a constant displacement can reduce dramatically roll RAOs of the drillship around the natural roll period under bow quartering waves and beam waves, respectively. The coupling effect of roll and heave leading to the heave RAOs decreasing around the natural roll period in beam waves, as well as coupling effect in heave, pitch and roll motion RAOs around the natural roll period in bow quartering waves are observed in the experimental results. The results presented in this study can provide references to the design of the moonpool of a drillship.

1. Introduction

Drillships are one of the important equipment for the exploration and development of offshore oil and gas resources. As a drillship possesses a boat-like structure, it is more suitable for ultra-deep water (water depth>1500m) operations with good manoeuvrability, large variable loads and strong self-holding ability compared to other structure forms. However, the ship-like structure of a drillship may be significantly affected by waves and is sensitive to wave direction. In addition, the middle part of a drillship generally has a moonpool structure through the hull from the main deck to the bottom. Under the action of external waves, the fluid in the moonpool is prone to suffer gap resonance, which may cause violent sloshing and piston motions of the fluid in the moonpool and thus has an important impact on the motion performance of the drillship and the safety of operation of the drilling equipment and crew. Therefore, the study on hydrodynamic performance of a drillship is of great practical significance to ensure safe operation of a drillship.

Over the past several decades, many researchers have carried out studies on the hydrodynamic performance of drillships. Fukuda (1977) studied behaviour of water in the moonpool of a drillship and its effects on the ship motion, and subsequently proposed empirical formulas for calculating resonant frequencies of a moonpool. Faltinsen (1993) derived an analytical formula for the resonant frequency of piston-mode motion of the fluid within a circular moonpool in the framework of linear theory. Molin (2001, 2017) and Molin et al. (2018) presented quasi-analytical expressions for solving resonant frequencies of piston and sloshing motions of the fluid within a moonpool. The above formulas are based on some assumptions, and could have some deviations from corresponding model test results. Fredriksen et al. (2015) investigated the resonant piston-mode motion in the moonpool and rigid-body motions. It is found that the moonpool strongly affects heave motions in a frequency range around the piston-mode resonance frequency of the

* Corresponding author.
E-mail address: longbin.tao@strath.ac.uk (L. Tao).

https://doi.org/10.1016/j.oceaneng.2022.112241
Received 11 April 2022; Received in revised form 5 August 2022; Accepted 7 August 2022
Available online 27 August 2022

Table 1
Main particulars of the drillship.

Items	Symbol	Unit	Full scale
Length between perpendiculars	L_{pp}	m	168.0
Breadth	B	m	32.0
Depth	D	m	15.5
Displacement	△	t	41315.1
Longitudinal position of centre of gravity from the after perpendicular	LCG	m	81.72
Vertical position of centre of gravity from baseline	VCG	m	13.03
Radius of gyration in roll	R_{xx}	m	13.244
Radius of gyration in pitch	R_{yy}	m	46.243

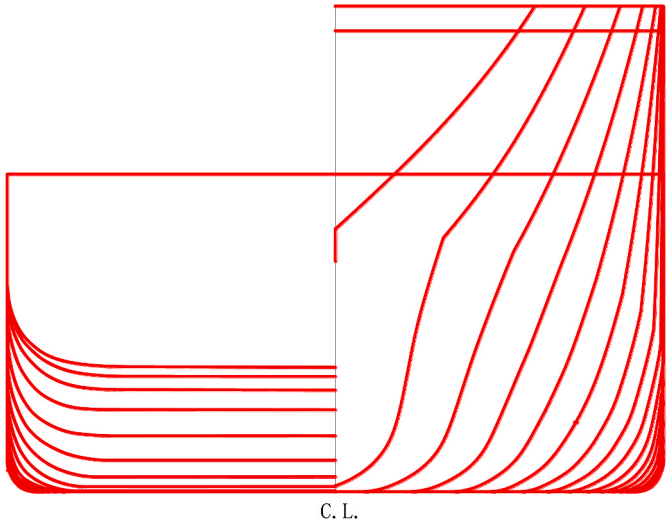

Fig. 1. Body plan of the drillship.

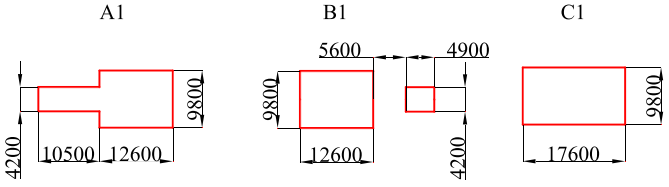

Fig. 2. Schematic diagrams of moonpools with different shapes (Reference size) (Unit: mm).

Table 2
Drafts corresponding to different moonpools.

Moonpool type	Label	Draft(m)
Conjoined double moonpool	A1	9.200
	A2	9.360
	A3	8.995
Separated double moonpool	B1	9.111
	B2	9.311
	B3	8.989
Single rectangular moonpool	C1	9.160
	C2	9.395
	C3	8.989

moonpool. It is also pointed out that no resonant water motions occur in the moonpool at the piston-mode resonance frequency, and instead large moonpool motions occur at a heave natural frequency associated with small damping near the piston-mode resonance frequency. Sivabalan and Surendran (2017) studied the hydrodynamic performance of a moonpool with variable section by numerical simulation and model test, respectively and analysed the influence of the tilt angle of the front-end face of a moonpool on the hydrodynamic performance of a drillship.

Wei et al. (2011) studied the influence of the change in the size of a rectangular moonpool of an FDPSO on its hydrodynamic performance by numerical simulation and model test, respectively. Sun (2013) carried out numerical simulation and model test research on a drillship with a rectangular moonpool with steps, and studied the influence of the resonant piston motion of the moonpool on the motion performance of the drillship. Liu and Zhang (2013) studied the motion performance of a deep-water drillship by numerical simulation and model test, and analysed the influence of a moonpool on the motion performance of the drillship. It is shown that the existence of the moonpool can significantly increase rolling motion of the drillship in beam waves. Guo et al. (2016) studied hydrodynamic performance of a deep-water drillship with a rectangular moonpool with steps through numerical simulation and model test, and analysed the resonance frequency of the fluid inside the moonpool. Zhang et al. (2016) studied the adaptability of a drillship in offshore operation by means of numerical simulation and model test. The effects of rectangular, circular and square moonpools on the motion performance of the drillship are analysed. It is indicated that the change in the shape of a moonpool has significant influence on the RAOs around the natural frequency of the piston motion of the water inside the moonpool.

Chen et al. (2018) used AQWA software to carry out hydrodynamic analysis of a drillship with a circular and square moonpool, respectively. Using HydroStar, Zhang et al. (2018) studied the influence of moonpool resonance on the motion performance of a drillship with a rectangular moonpool and a rectangular moonpool with steps, respectively and analysed the difference between the numerical and theoretical solutions of the resonant frequencies of the piston and sloshing motion of the drillship. It is demonstrated that the piston resonance motion of the moonpool can increase the heave motion of the drillship. Song et al. (2018) analysed the influence of a moonpool on the motion RAOs and added mass coefficients of a drillship by numerical simulation and model test. It is shown that the added mass of the fluid in the moonpool can change dramatically when the moonpool resonance occurs. Xianyu and Lv (2018) studied the hydrodynamic performance of a drillship and the fluid motion in the moonpool by computational fluid dynamics (CFD), potential flow theory and model test, respectively.

Most of the aforementioned studies consider rectangular or circular moonpools, and the draft is assumed to remain unchanged when the size of a moonpool changes, which results in the change in displacement. In actual design process, the certain displacement of a drillship is helpful to maintain the stable storage capacity of drilling equipment and beneficial to determine the economic sailing speed of the ship,and it is possible to optimize the shape and size of a moonpool under the same displacement. The objective of this paper is to conduct numerical and experimental study on the influence of the shape and size of a moonpool on the motion performance and stability of a drillship under a certain displacement. In the case of the certain displacement, this study first carried out the hydrostatic calculation of the drillship of different sizes of a conjoined double moonpool, separated double moonpool and single rectangular moonpool, respectively. The GZ curves and the drafts of the drillship with the moonpools of different shapes and sizes are obtained. Under the corresponding drafts, the hydrodynamic analyses were carried out based on three-dimensional (3D) potential flow theory to obtain the motion RAOs of the drillship with the moonpools of different shapes and sizes under the conditions of head waves, bow quartering waves and beam waves, respectively and the influence of the change in the shape and size of the moonpool on the motion performance of the drillship was analysed in depth. Model tests were carried out to validate the corresponding numerical results of the motion RAOs of the drillship with a conjoined double moonpool.

The present paper is organized as follows. The calculation of the GZ curves is given in Section 2 following Introduction. The detailed numerical simulation results of the motion RAOs of the drillship and

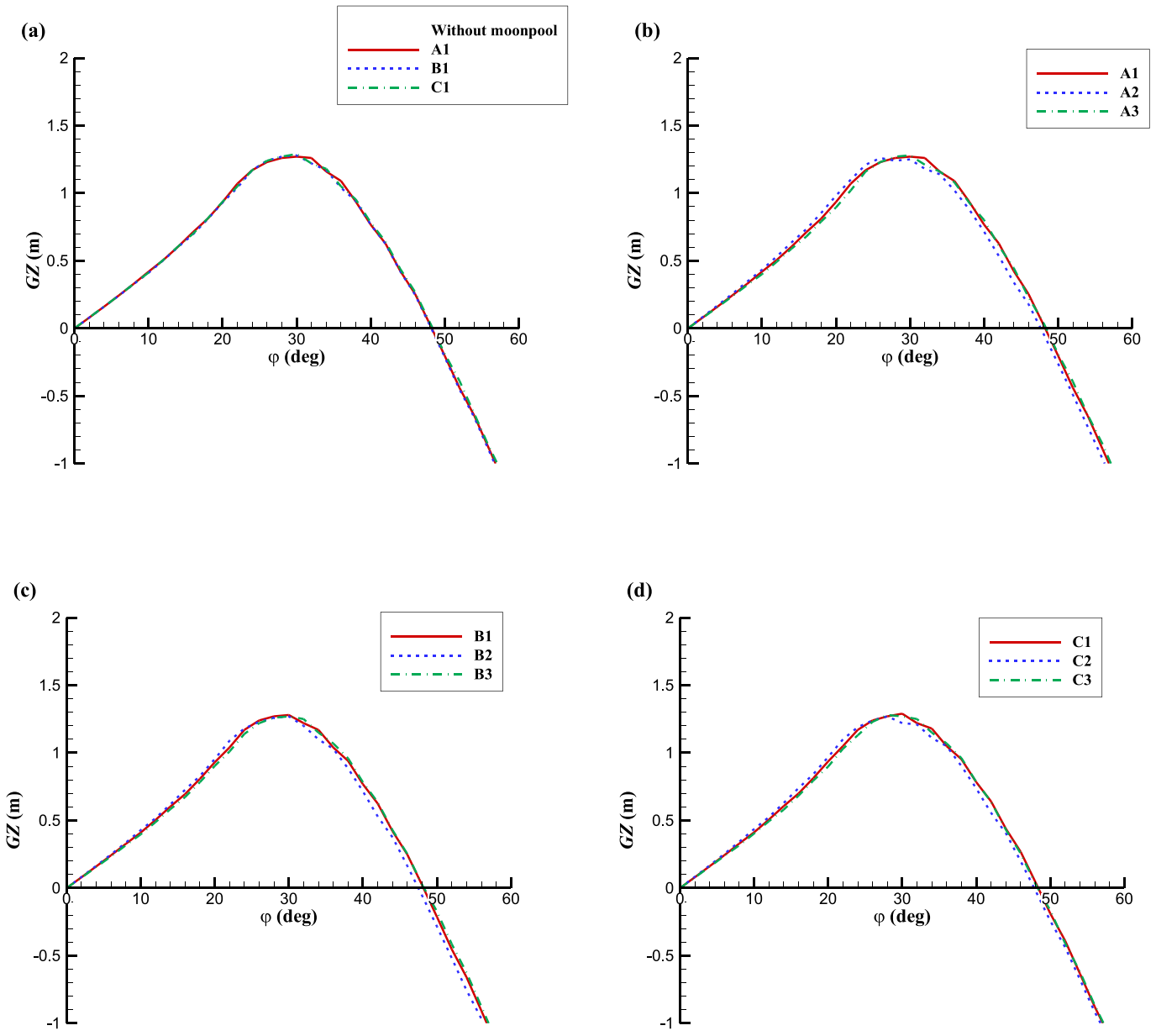

Fig. 3. Static stability curves of the drillship with the moonpool of different shapes and sizes: (a) Comparison of the moonpool with different shapes; (b) Comparison of the conjoined double moonpool of different sizes; (c) Comparison of the separated double moonpool of different sizes; (d) Comparison of the single rectangular moonpool of different sizes.

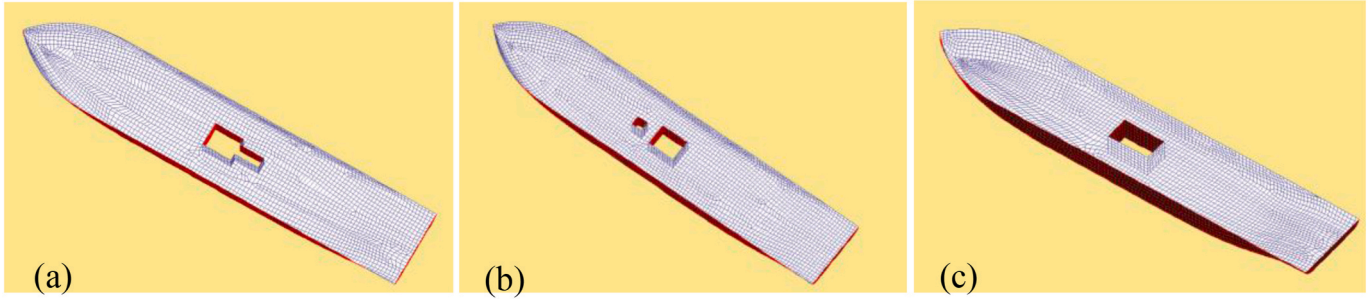

Fig. 4. HydroStar hydrodynamic calculation mesh models of the drillship with the moonpools of a reference size:
(a) conjoined double moonpool; (b) separated double moonpool; (c) single rectangular moonpool.

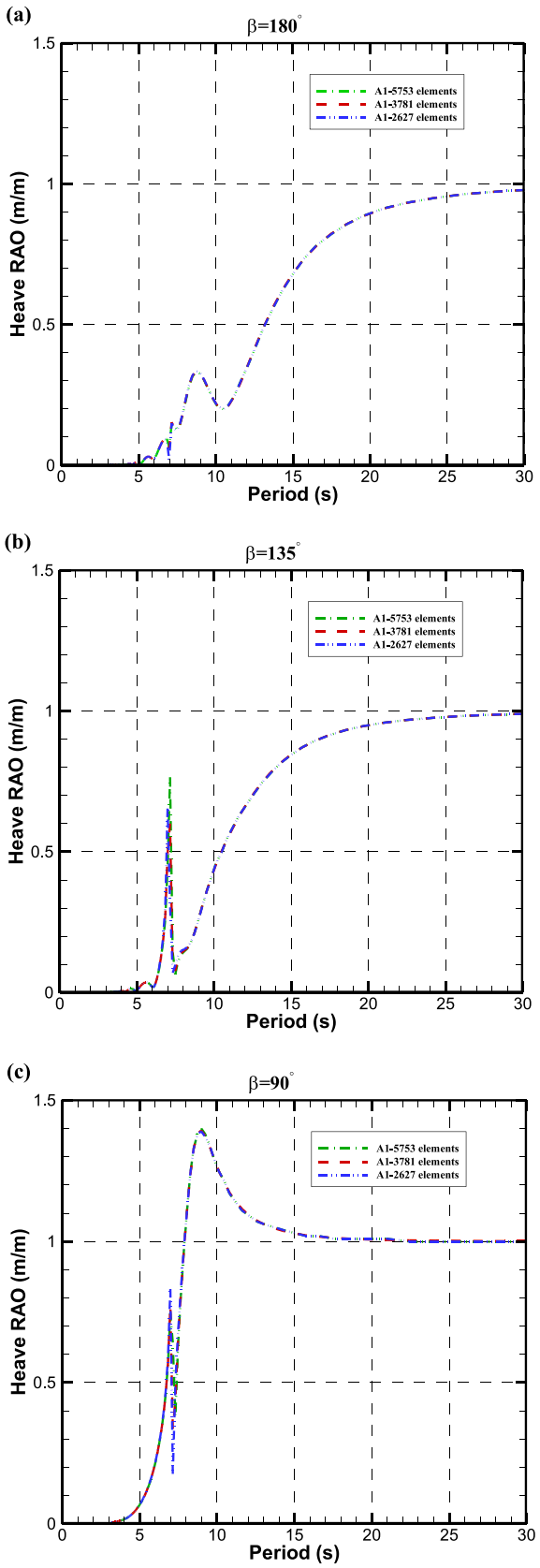

Fig. 5. Heave RAOs of the drillship with the A1 moonpool by different calculation elements.

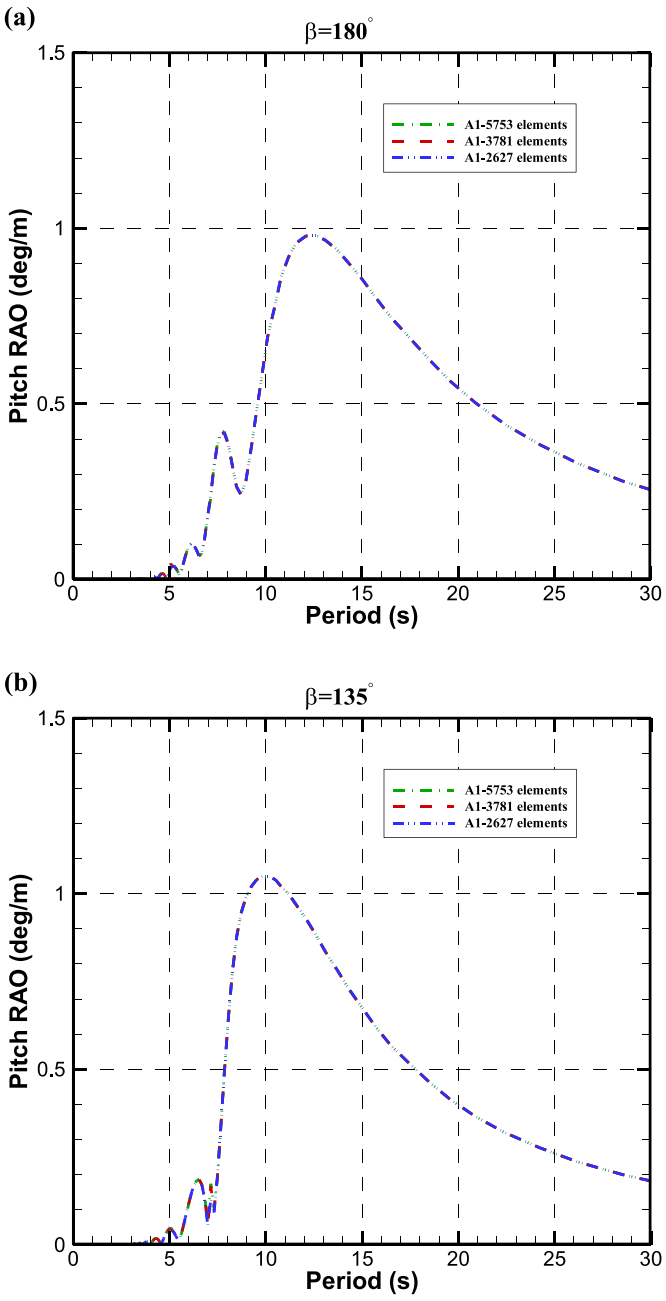

Fig. 6. Pitch RAOs of the drillship with the A1 moonpool by different calculation elements.

further analyses on the influence of different shapes and sizes of a moonpool are presented in Section 3. The RAO results of the model tests of the drillship with a conjoined double moonpool and the comparison with the corresponding numerical results are provided in Section 4. Finally, conclusions are drawn based on the present study.

2. Calculation of static stability curve

Based on the theory of ship hydrostatics (Sheng et al., 1992), a program was developed to calculate GZ curves of the drillship with a moonpool of different shapes and sizes. The main particulars of the drillship are shown in Table 1. Fig. 1 shows the body plan of the drillship. Fig. 2 shows the schematic diagrams of the moonpool with different shapes (reference size), which are the reference size conjoined double moonpool (A1), reference size separated double moonpool (B1)

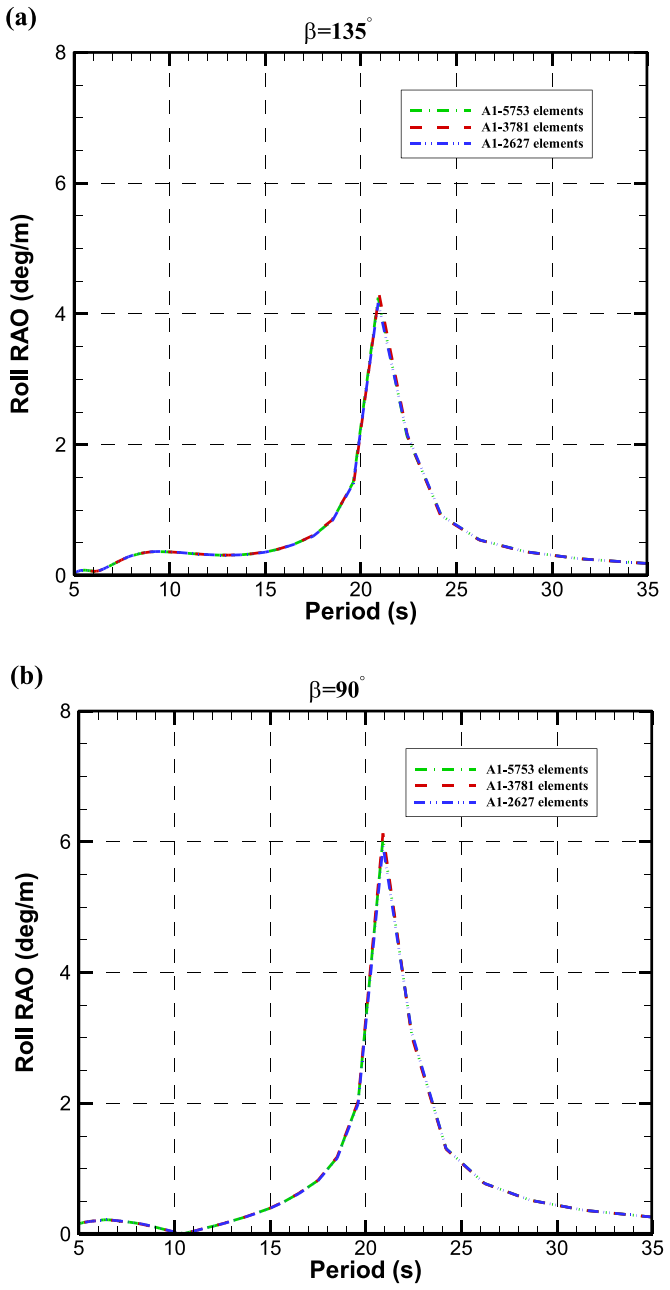

Fig. 7. Roll RAOs of the drillship with the A1 moonpool by different calculation elements.

and reference size single rectangular moonpool (C1).

Table 2 shows the drafts of the drillship with a moonpool of different shapes and sizes in the case of a constant displacement. It can be seen that the draft corresponding to the reference size (A1) of the conjoined double moonpool is 9.2m. When each length of the sides of the moonpool (A2) increases to 1.3 times that of the A1 moonpool, the draft of the drillship increases to 9.36m. When each length of the sides of the moonpool (A3) decreases to 0.7 times that of the A1 moonpool, the draft of the drillship decreases to 8.995m. It is seen that under the condition of the constant displacement, the larger the opening size of the moonpool, the larger the draft. The variable trend of the draft of the drillship with the separated double moonpools and single rectangular moonpools is similar to that of the conjoined double moonpool when each length of the sides of the corresponding moonpool increases or decreases.

Fig. 3(a) shows the comparison of the GZ curves of the drillship with the moonpool of different shapes and sizes. It can be seen that there is

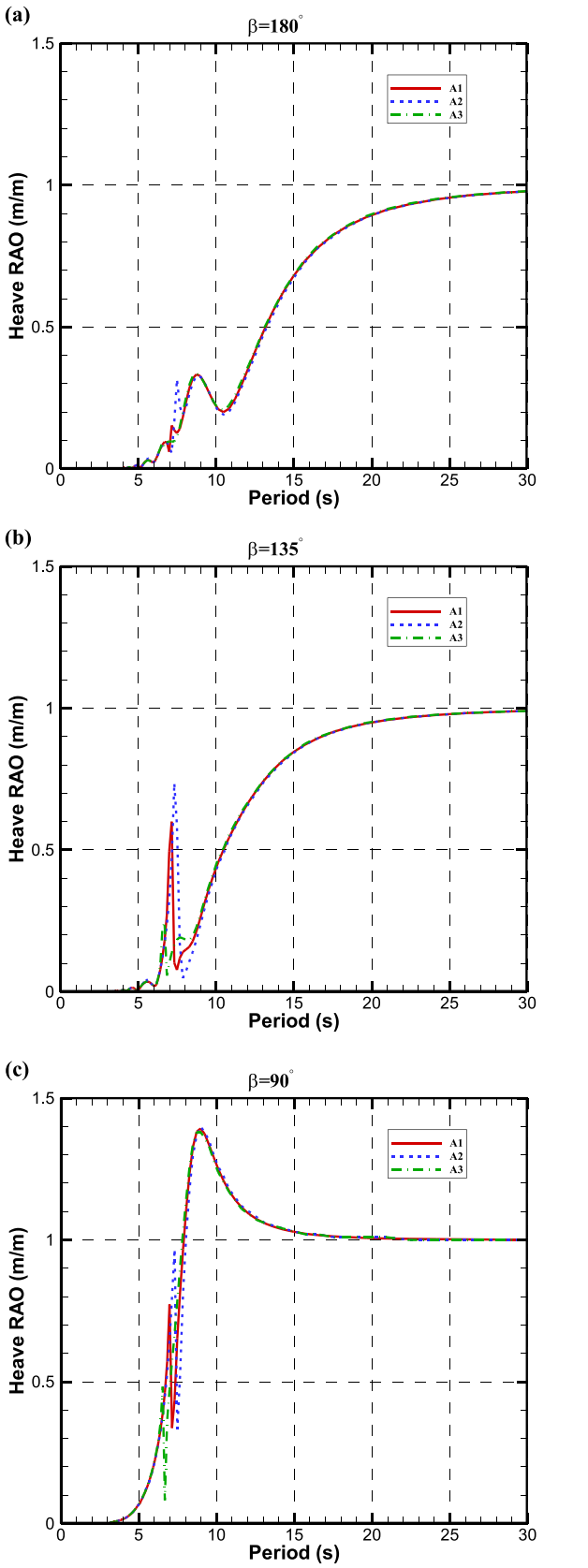

Fig. 8. Comparison of the numerical results of the heave motion RAOs for the drillship with the conjoined double moonpool of different sizes.

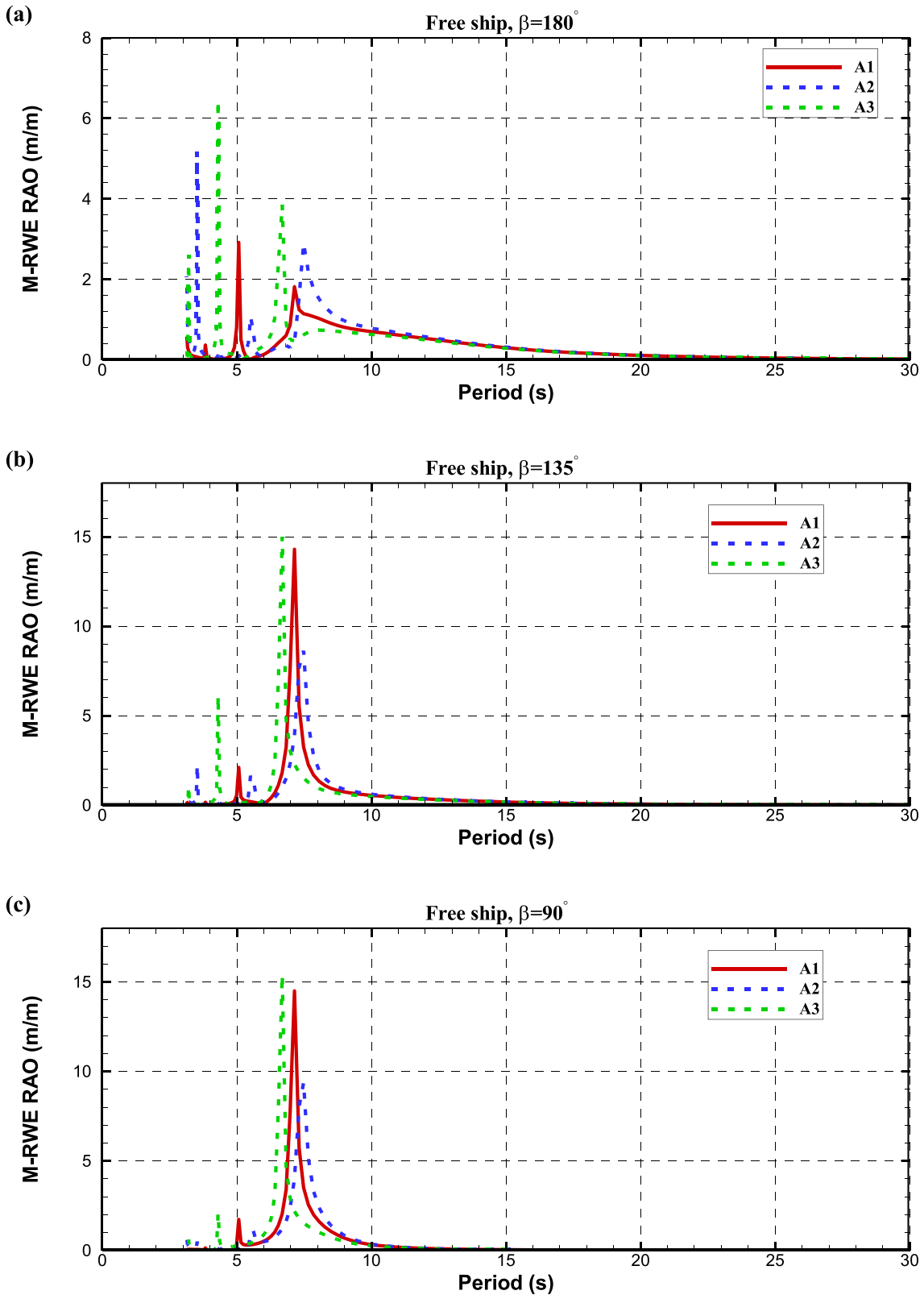

Fig. 9. RAOs of relative wave elevation around the middle of the conjoined double moonpool of different sizes at different wave headings for the drillship free to respond to incident waves.

slight difference in the GZ curves of the drillship with the different moonpool shapes in reference size. Due to the increase in the draft caused by the opening of the moonpool, the restoring arm of the drillship with a moonpool is larger than that of the drillship without a moonpool over the range of heeling angle (φ) from 0 to 35°. The maximum increment is approximately 8% when $\varphi = 30°$. Fig. 3(b)–(d) show the comparison between the GZ curves of the drillship of different sizes for each type of the moonpool considered, respectively. It can be

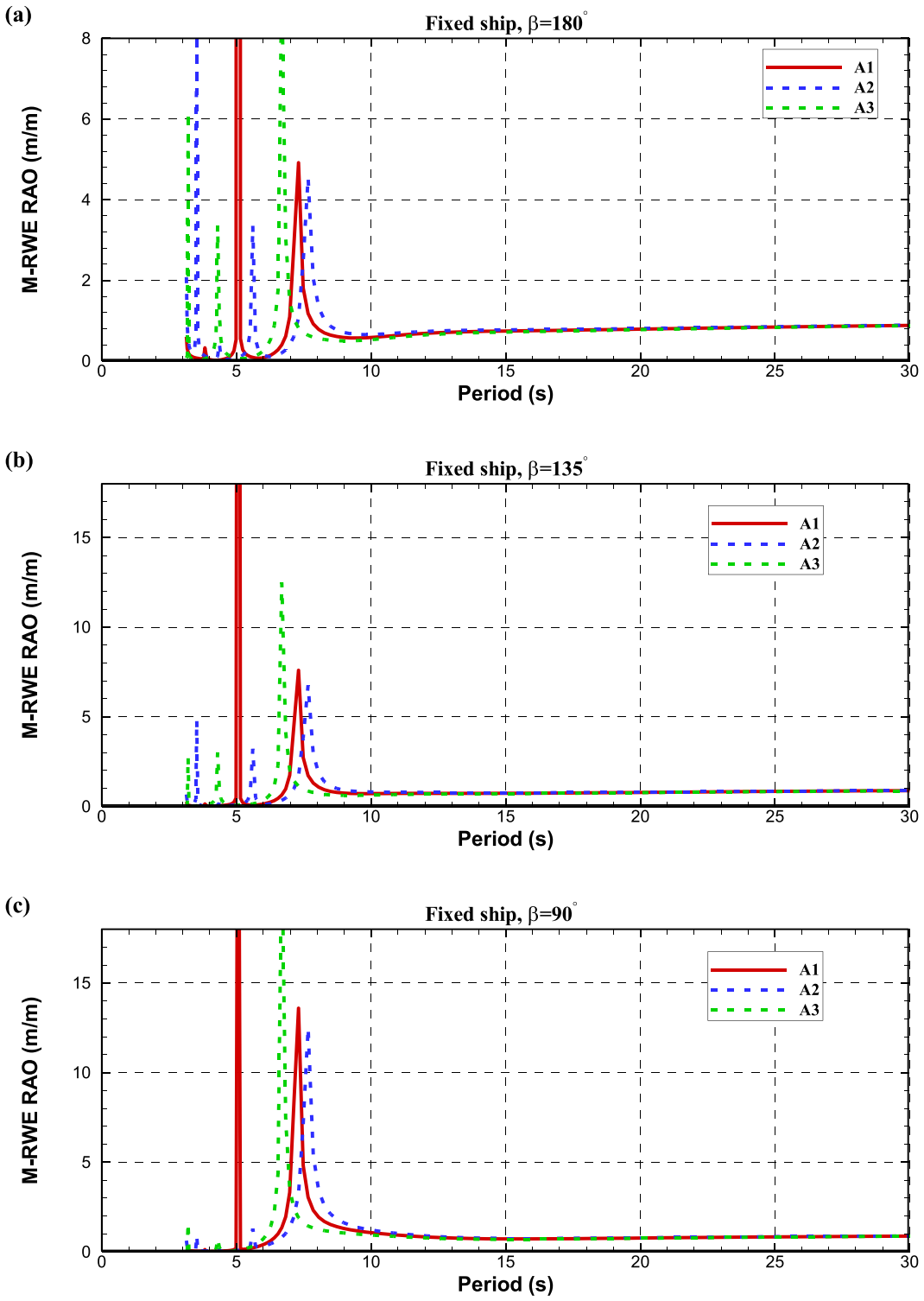

Fig. 10. RAOs of relative wave elevation around the middle of the conjoined double moonpool of different sizes at different wave headings for the drillship fixed in incident waves.

seen that when $0° < \varphi < 27°$, the larger the opening of the moonpool, the larger the GZ values; When $\varphi > 27°$, the smaller the opening of the moonpool, the larger the GZ values. The variation in the opening size of the moonpool holds slighter effect on the GZ curves of the drillship.

3. Numerical simulation of motion performance

Based on the drafts obtained by the hydrostatic calculation of the drillship with different moonpools in the case of the constant displacement, the hydrodynamic commercial software HydroStar developed by Bureau Veritas (BV) is employed to carry out numerical simulation study on the motion performance of the drillship in the wave direction of head waves, bow quartering waves and beam waves, respectively.

Table 3
Peak periods of the M-RWE RAOs for the free ship and fixed ship with the conjoined double moonpool.

Moonpool Type	Peak period of M-RWE RAOs	Free ship			Fixed ship		
		$\beta = 180°$	$\beta = 135°$	$\beta = 90°$	$\beta = 180°$	$\beta = 135°$	$\beta = 90°$
A1	T_0 (s)	7.14	7.14	7.14	7.31	7.31	7.31
	T_1 (s)	5.07	5.07	5.07	5.07	5.07	5.07
	T_2 (s)	3.83	3.83	3.83	3.83	3.83	3.83
A2	T_0 (s)	7.48	7.48	7.48	7.66	7.66	7.66
	T_1 (s)	5.51	5.51	5.61	5.61	5.61	5.61
	T_2 (s)	4.36	4.36	4.36	4.36	4.36	4.36
A3	T_0 (s)	6.68	6.68	6.68	6.68	6.68	6.68
	T_1 (s)	4.30	4.30	4.30	4.30	4.30	4.30
	T_2 (s)	3.21	3.21	3.21	3.21	3.21	3.21

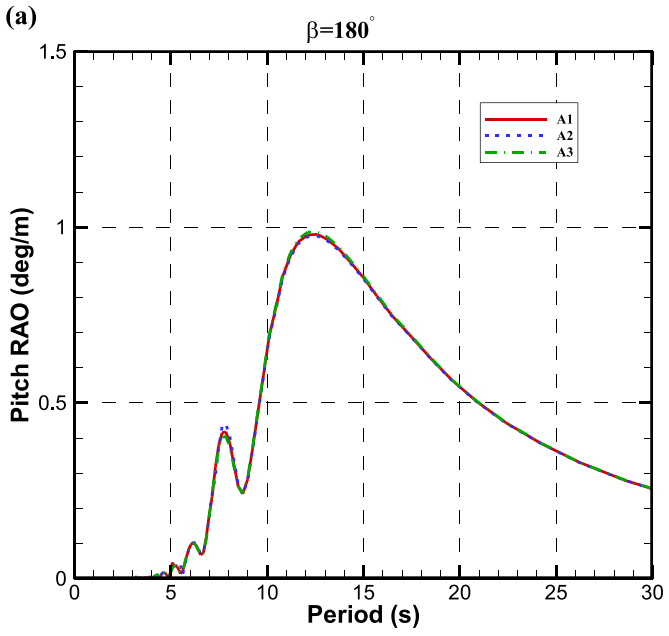

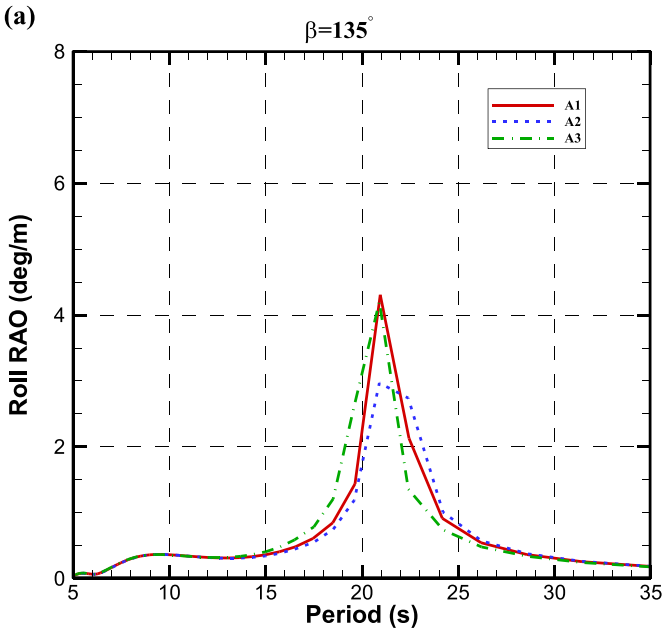

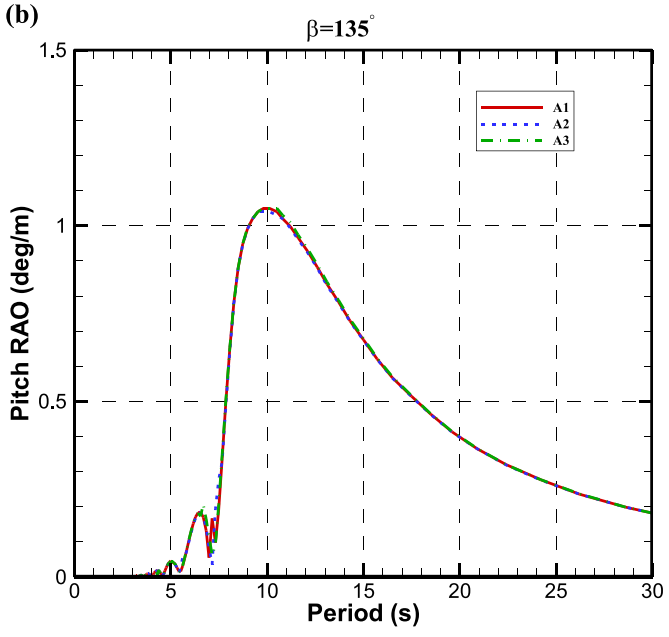

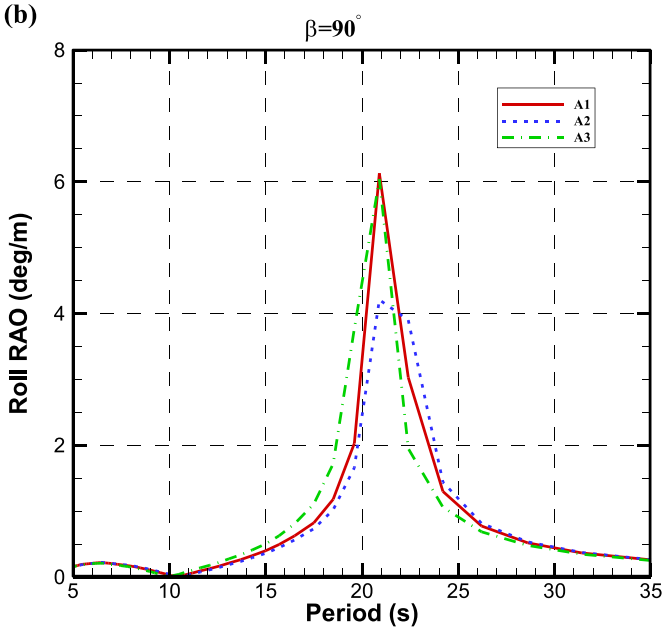

Fig. 11. Comparison of the numerical results of the pitch motion RAOs for the drillship with the conjoined double moonpool of different sizes.

Fig. 12. Comparison of the numerical results of the roll motion RAOs for the drillship with the conjoined double moonpool of different sizes.

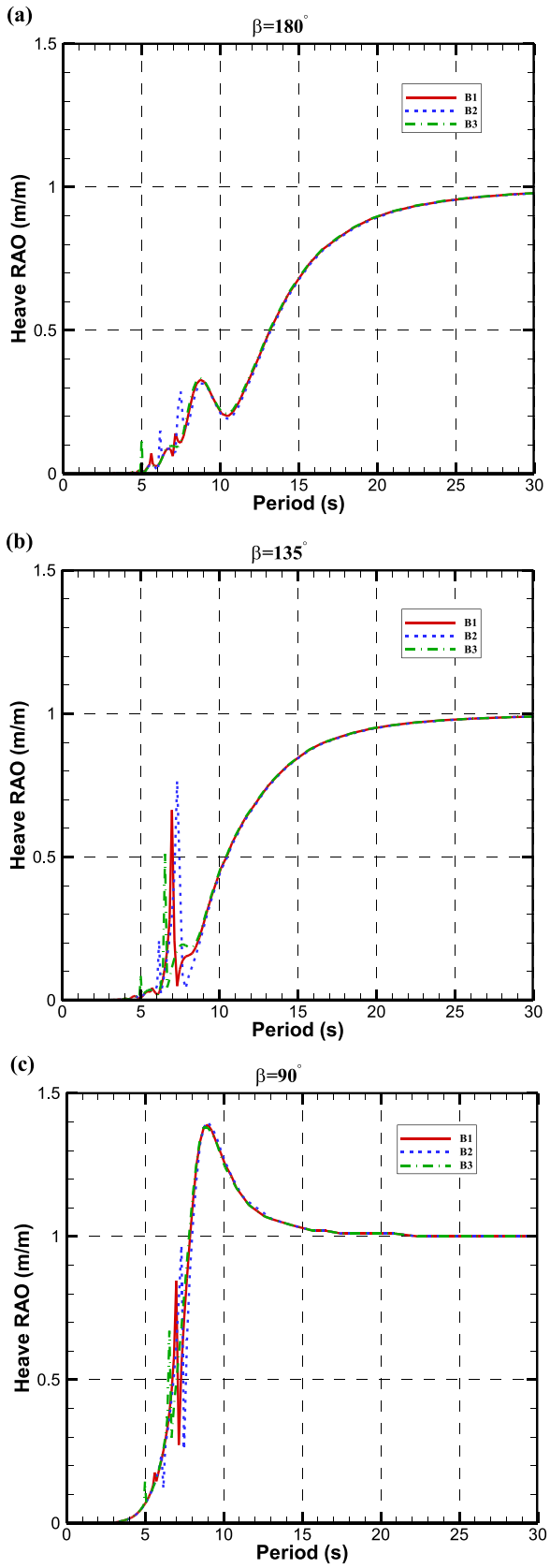

Fig. 13. Comparison of the numerical results of the heave motion RAOs for the drillship with the separated double moonpool of different sizes.

3.1. Introduction to HydroStar

HydroStar is a hydrodynamic calculation software based on three-dimensional potential flow theory in frequency domain. HydroStar can perform conventional hydrodynamic analysis of ships and offshore structures to obtain motion RAOs, velocity, acceleration, and relative motion, etc. In the process of analysis, HydroStar can eliminate irregular frequencies and take the energy dissipation of a moonpool into account.

3.2. Hydrodynamic model

The hydrodynamic calculation based on HydroStar first requires to establish a finite element mesh model. In this study, the finite element mesh model of the drillship was established by Patran, and then imported to HydroStar to perform hydrodynamic analysis. Fig. 4(a)-(c) show the hydrodynamic calculation mesh models of the three types of moonpool shape of the drillship, respectively.

3.3. Calculation settings

The diffraction/radiation calculation to obtain the hydrodynamic coefficients, i.e., added mass and radiation damping, was carried out in frequency domain. The frequency range of the regular waves selected in the diffraction/radiation calculation is 0.1–2 Hz. In order to capture the resonant frequency of the moonpool, the frequency step is set as 0.02 Hz, with a total of 96 frequencies. The wave heading angle β is selected as 180° (head waves), 135° (bow quartering waves) and 90° (beam waves), respectively. According to the model test results of the drillship with a conjoined double moonpool in the following experimental study, the roll viscous damping of the drillship is set as 2.2% of the critical damping in the motion calculation.

3.4. Mesh independence study

To verify the influence of mesh element number on the numerical results, the drillship with the A1 moonpool is utilized to conduct the numerical simulation of motion performance. The length of an element is selected as 1.8m, 1.5m and 1.2m, corresponding to 2627, 3781 and 5753 elements, respectively. Figs. 5–7 shows the heave, pitch and roll RAOs of the drillship with the A1 moonpool by different calculation elements at different wave headings, respectively. It can be seen that the agreement of the heave RAOs by the different elements is satisfactory. The peaks and corresponding periods can be exactly captured although there exist some rather slight discrepancies for the element number of 2627. In consideration of accuracy and efficiency of the numerical simulations, the length of an element is determined as 1.5 m for all the numerical simulations.

3.5. Calculation results

The hydrodynamic analysis was carried out to obtain the motion RAOs of the drillship with the moonpool of different shapes and sizes under the conditions of head waves, bow quartering waves and beam waves, respectively.

3.5.1. Conjoined double moonpool

Fig. 8 shows the comparison of the numerical results of the heave motion RAOs for the drillship with the conjoined double moonpool of different sizes at different wave headings. The heave RAOs in head waves for each case in Fig. 8(a) have two evident peaks. The peak around 8.7s is caused by the resonant heave motion of the ship, and the different sizes of the moonpool appear to have almost no influence on this peak. The other peaks around 7.1s, 7.5s and 6.5s for Cases A1, A2 and A3 respectively, are caused by the near resonant piston mode water motion inside the moonpool, and the different sizes of the moonpool have notable influence on both the value and corresponding period of

Table 4
Peak periods of the M-RWE RAOs for the free ship and fixed ship with the separated double moonpool.

Moonpool Type	Peak period of M-RWE RAO	Free ship			Fixed ship		
		$\beta = 180°$	$\beta = 135°$	$\beta = 90°$	$\beta = 180°$	$\beta = 135°$	$\beta = 90°$
B1-L	T_0 (s)	7.14	6.98	6.98	7.14	7.14	7.14
	T_1 (s)	5.61	5.61	5.71	5.61	5.61	5.71
	T_2 (s)	3.93	3.93	3.93	–	–	–
B2-L	T_0 (s)	7.48	7.31	7.31	7.48	7.48	7.48
	T_1 (s)	6.16	6.16	6.16	6.16	6.16	6.16
	T_2 (s)	3.21	3.21	3.21	3.21	3.21	3.21
B3-L	T_0 (s)	6.55	6.55	6.55	6.68	6.68	6.68
	T_1 (s)	4.99	4.99	4.99	4.99	4.99	4.99
	T_2 (s)	–	–	–	–	–	–
B1–S	T_0 (s)	5.61	5.61	5.61	5.61	5.61	5.61
	T_1 (s)	3.93	3.93	3.93	3.93	–	3.93
	T_2 (s)	–	–	–	–	–	–
B2–S	T_0 (s)	6.16	6.16	6.16	6.16	6.16	6.16
	T_1 (s)	4.42	4.42	–	4.42	4.49	4.49
	T_2 (s)	–	–	–	–	–	–
B3–S	T_0 (s)	4.99	4.99	4.99	4.99	4.99	4.99
	T_1 (s)	3.27	3.27	3.27	3.27	3.27	3.27
	T_2 (s)	–	–	–	–	–	–

these peaks. In order to further clarify the relationship between these RAO peaks and the water motion inside the moonpool, the RAOs of the relative wave elevation around the middle of the conjoined double moonpool (M-RWE) of different sizes at different wave headings for the drillship free to respond to incident waves and for the drillship fixed in incident waves are shown in Fig. 9 and Fig. 10, respectively. The piston and sloshing mode resonant periods can be obtained from the peak periods for the drillship fixed in incident waves as shown in Fig. 10. The peak periods of the M-RWE RAOs denoted as T_0, T_1, and T_2 from large to small for the free and fixed drillship with the conjoined double moonpool respectively are shown in Table 3. It can be seen that the heave motion RAO peak periods for Cases A1 and A2 (7.1s and 7.5s) are equal to those of the M-RWE RAOs of the drillship free to respond to incident waves. These periods are slightly lower than the piston mode resonant periods obtained by the fixed drillship in incident waves. A similar trend was also reported by Fredriksen et al. (2015). The heave motion RAO peak period for Case A3 (6.5s) is slightly different from the peak period (6.68s) of the M-RWE RAOs of the drillship free to respond to incident waves. It is also seen that for Case A3 with a smaller moonpool size, the peak period T_0 for the free ship has the same value as the piston mode resonant period for the fixed ship, which is different with the conclusion of Fredriksen et al. (2015). As pointed out by Newman (2018), the interaction between heave and piston mode could be exaggerated in two-dimensional (2D) case, which is similar to the barge with a moonpool that extends throughout the entire length of the hull in Fredriksen et al. (2015). It is indicated at least for the present configurations, the changes in the resonant periods (<3%) are rather small. Moreover, it can also be seen in Table 3 that the larger the size of the moonpool, the larger the piston mode resonant period. The heave motion RAOs for each case have a peak around the resonant piston period due to the added mass A_{33} being directly affected by the resonant or near resonant piston mode water motion (Mavrakos, 1988; Yeung and Seah, 2007; Kawabe et al., 2010; Han et al., 2022). The different heave motion RAOs peak values for Cases A1, A2 and A3 around their piston mode resonant periods respectively are mainly dependent on combined interaction between heave exciting force, added mass and radiation damping.

With the wave direction ranging from 180° to 90°, the heave motion RAOs is enhanced. It can be seen in Fig. 8(b) that only one peak arises around 7.1s, 7.5s and 6.5s for Cases A1, A2 and A3 respectively, resulting from the near resonant piston mode water motion inside the moonpool. It is worth noting that different from the RAOs in head waves, no notable peak around 8.0s arises mainly due to the lower heave exciting force level resulting from the cancellation effects induced by the phase difference of the heave exciting force along the drillship direction as presented in Faltinsen (1993). As shown in Fig. 8(c), the RAOs for each case have two rather sharper peaks compared to those in Fig. 8(a). The occurrence periods of the peaks caused by the near resonant piston mode water motion are almost the same as those in head waves and bow-quartering waves. The different sizes of the moonpool have almost no influence on the heave RAOs around the heave resonance period (about 8.5s). The pronounced resonant heave RAO peaks are due to the beam waves with the period equal to the natural heave period have intense disturbance force on the heave motion of the ship.

Fig. 11 shows the comparison of the numerical results of the pitch motion RAOs for the drillship with the conjoined double moonpool of different sizes at different wave headings. Each case in Fig. 11(a) has several peaks. The peak around 12s is caused by the waves with the wavelength comparable to the ship length, leading to intense disturbance to the ship in head waves. The smaller peak around 8s is caused by the resonant pitch motion due to lower exciting level resulting from cancellation effects. The peaks around 5s are caused by the near resonant or resonant 1st order sloshing mode water motion as shown in Table 3. Besides, it is clearly seen that the change in the opening size of the moonpool has almost no influence on the pitch motion RAOs. This is due to the change in the opening size of the moonpool merely leads to slight change in the wave disturbance force, added inertia moment, damping as well as restoring stiffness in pitch mode. The pitch RAOs in bow quartering waves in Fig. 11(b) have similar features compared to those in head waves. The main discrepancy is the smaller peak period (approximate 10s). According to linear dispersion relation, the projection of the wavelength of the regular wave with the period T equal to 10s on the direction of the drillship is approximately 220.6m ($1.56T^2/cos45°$), which is very close to the wavelength (224.6m) with the period T equal to 12s inducing the maximum pitch motion RAO of the ship in head waves. This is why the pitch RAO of the drillship in bow-quartering waves has a smaller peak period (about 10s) compared to that (about 12s) of the drillship in head waves. Besides, no evident peak appears around the natural pitch period (about 8s) in Fig. 11(b) since the exciting level at 8s is not significantly higher than that at adjacent periods resulting from cancellation effects.

Fig. 12 shows the comparison of the numerical results of the roll motion RAOs for the drillship with the conjoined double moonpool of different sizes at different wave headings. As can be seen, the difference of the roll RAOs between the reference size (A1) and smaller size (A3) of the moonpool of the drillship is slight. When the opening of the moonpool increases to the larger size (A2), the roll motion RAOs around the natural roll period of the drillship in bow-quartering waves and beam waves decrease by approximately 25% and 30%, respectively. This is

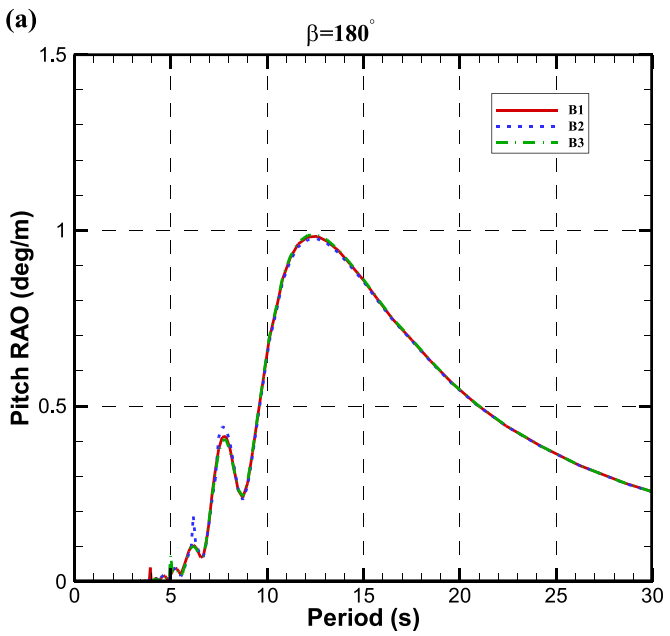

Fig. 14. Comparison of the numerical results of the pitch motion RAOs for the drillship with the separated double moonpool of different sizes.

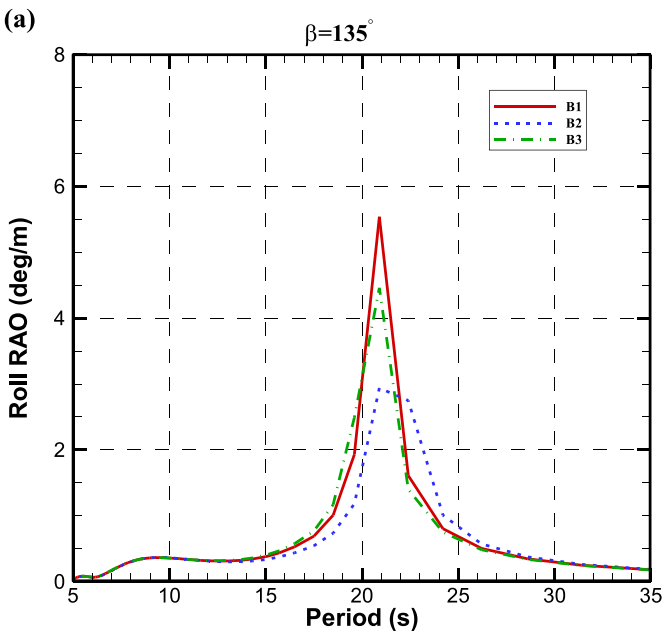

Fig. 15. Comparison of the numerical results of the roll motion RAOs for the drillship with the separated double moonpool of different sizes.

mainly due to that larger size of the opening of the moonpool under the condition of the constant displacement leads to increase in the draft, which can significantly increase the added inertial moment of roll at the natural roll period. While for A3, i.e. the smaller opening with a smaller draft, the decrease in the added inertial moment of roll and the increase in roll radiation damping cause jointly the roll RAO around the natural roll period slightly different with that of the drillship with the A1 moonpool.

3.5.2. *Separated double moonpool*

Fig. 13 shows the comparison of the numerical results of the heave motion RAOs for the drillship with the separated double moonpool of different sizes at different wave headings. The feature of the heave motion RAOs for the drillship with the separated double moonpool is similar to that for the drillship with the conjoined double moonpool. Since the separated double moonpool contains two individual moonpools, each case has two peaks ranging from 5s to 8s due to the near resonant or resonant piston mode water motion inside the moonpool. Table 4 shows the peak periods of the M-RWE RAOs denoted as T_0, T_1, and T_2 from large to small for the free and fixed drillship with the separated double moonpool, respectively. It can be seen that the changes in the peak period of the M-RWE RAOs for the larger individual moonpool (B1-L, B2-L, B3-L) of each separated double moonpool for the free drillship and fixed drillship is still rather small. For the smaller individual moonpool (B1–S, B2–S, B3–S) of each separated double moonpool, the peak period almost remains constant.

It can be observed in Fig. 13(a) that the larger and smaller heave peak periods of Case B1 are approximately 7.1s and 5.6s, respectively,

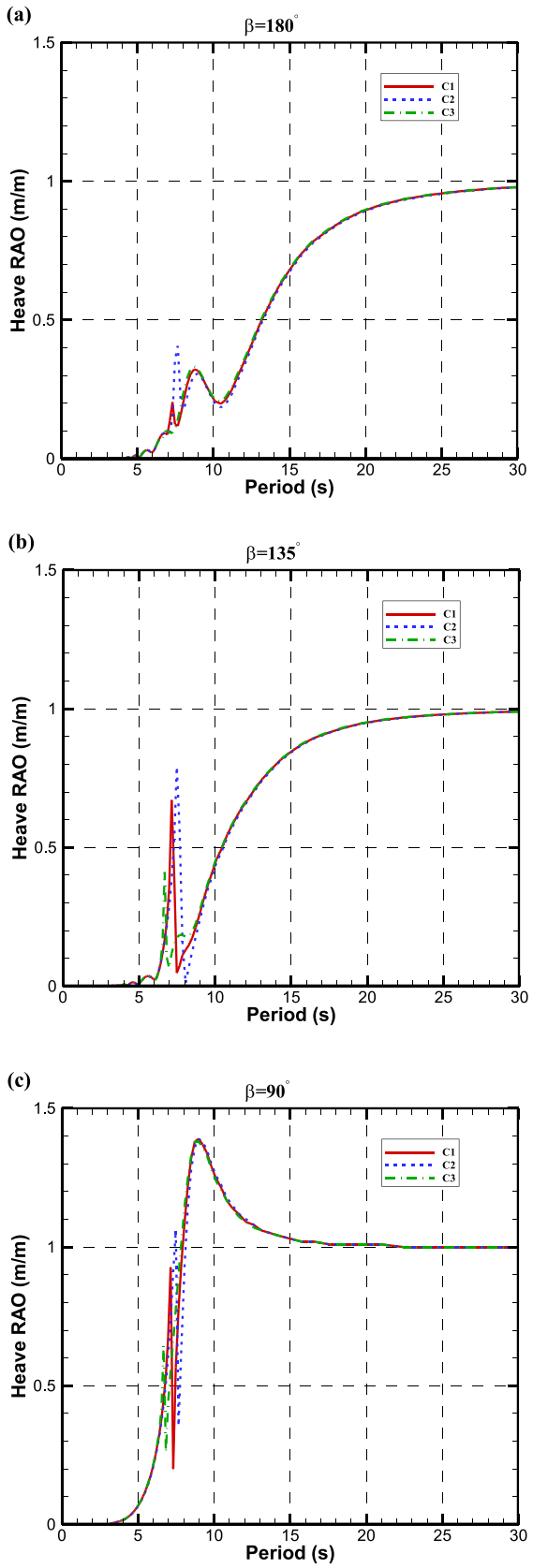

Fig. 16. Comparison of the numerical results of the heave motion RAOs for the drillship with the single rectangular moonpool of different sizes.

which are consistent with T_0 for B1-L and B1–S in Table 4. The larger and smaller heave peak periods of Case B2 are approximately 7.5s and 6.2s, respectively, which are consistent with T_0 for B2-L and B2–S in Table 4. Moreover, the larger and smaller heave peak periods of Case B3 are approximately 6.8s and 5.0s, respectively. The larger peak period (6.8s) is slightly different with T_0 for B3-L (6.55s) in Table 4. This is due to the heave exciting force level around 6.55s is lower compared to adjacent values. The smaller peak period (5.0s) on the other hand is rather consistent with T_0 for B3–S (4.99s) in Table 4. It is also seen in Fig. 13(b) and (c) that the larger and smaller peak periods ranging from 5s to 8s of the heave motion RAOs in bow quartering and beam waves are in general consistent with T_0 in Table 4, respectively.

Fig. 14 shows the comparison of the numerical results of the pitch motion RAOs for the drillship with the separated double moonpool of different sizes at different wave headings. The feature of the pitch motion RAOs for the drillship with the separated double moonpool is also similar to that for the drillship with the conjoined double moonpool. Fig. 15 shows the comparison of the numerical results of the roll motion RAOs for the drillship with the separated double moonpool of different sizes at different wave headings. It can be seen that the roll motion RAOs around the natural roll period (about 21s) of the drillship with the separated double moonpool of the reference size (B1) is larger. The drillship with the separated double moonpool of the larger moonpool size B2 or the smaller moonpool size B3 has a smaller peak value of the roll motion RAO around the natural roll period. In fact, under the condition of the constant displacement, a larger size of opening with a larger draft can lead to increase in added inertial moment of roll and decrease in roll radiation damping around the natural roll period, while a smaller size of opening with a smaller draft can lead to decrease in added inertial moment of roll and increase in roll radiation damping around the natural roll period. The joint interaction of the two points leads to the smaller roll RAOs around the natural roll period for the drillship with the separated double moonpool of B2 and B3, respectively.

3.5.3. *Single rectangular moonpool*

Fig. 16 shows the comparison of the numerical results of the heave motion RAOs for the drillship with the single rectangular moonpool of different sizes at different wave headings. Table 5 shows the peak periods of the M-RWE RAOs denoted as T_0, T_1, and T_2 from large to small for the free and fixed drillship with the single rectangular moonpool, respectively. Similar to the drillship with the conjoined and separated double moonpools, the heave RAO peak periods ranging from 5s to 8s are consistent with T_0 for the free drillship in Table 5. The changes in the resonant periods are still rather small for the free drillship and fixed drillship as shown in Table 5. It is also seen that the change in the size of the moonpool has almost no influence on the heave motion RAO at other wave periods, as the influence of the change in the size of the rectangular moonpool on the heave added mass, damping as well as the heave disturbance force on the ship is slight.

Fig. 17 shows the comparison of the numerical results of the pitch motion RAOs for the drillship with the single rectangular moonpool of different sizes at different wave headings. Similar tendency compared to the drillship with the conjoined double and separated double moonpools can also be found. Moreover, it can be seen that the increase in the size of the single moonpool (Case C2) has relatively notable influence on the pitch motion RAOs peaks around 5 s for head waves in Fig. 17(a) and for bow quartering waves in Fig. 17(b), due to the decrease in the added inertial moment in pitch mode around the 1st order sloshing mode resonance period. Fig. 18 shows the comparison of the numerical results of the roll motion RAO for the drillship with the single rectangular moonpool of different sizes at different wave headings. It is also seen that the roll motion RAOs around the natural roll period of the drillship with the single rectangular moonpool of the reference size (C1) are larger, and both increase (C2) and decrease (C3) in the opening size can decrease the roll motion RAOs around the natural roll period. Similar to the aforementioned reason, this phenomenon can also be mainly

Table 5
Peak periods of the M-RWE RAOs for the free ship and fixed ship with the single rectangular moonpool.

Moonpool Type	Peak period of M-RWE RAO	Free ship			Fixed ship		
		$\beta = 180°$	$\beta = 135°$	$\beta = 90°$	$\beta = 180°$	$\beta = 135°$	$\beta = 90°$
C1	T_0 (s)	7.31	7.31	7.31	7.31	7.31	7.31
	T_1 (s)	4.62	4.62	4.55	4.62	4.62	4.62
	T_2 (s)	3.34	3.34	3.34	3.34	3.34	3.34
C2	T_0 (s)	7.66	7.66	7.66	7.85	7.85	7.85
	T_1 (s)	5.15	5.15	5.15	5.24	5.24	5.15
	T_2 (s)	3.79	3.79	3.79	3.79	3.79	3.79
C3	T_0 (s)	6.68	6.68	6.68	6.83	6.83	6.83
	T_1 (s)	3.88	3.88	3.88	3.88	3.88	3.88
	T_2 (s)	–	–	–	–	–	–

Table 6
Heave RAOs deviation between the experimental results and numerical results.

Wave heading	Period (s)	Exp. of Heave RAO of A1 (m/m)		Num. of	Absolute value of deviation (m/m)	
		Regular waves	WN waves		regular waves & WN waves	Exp. (regular waves) & Num.
180°	24.03	1.080	1.114	0.949	0.034	0.131
	21.50	1.066	1.037	0.920	0.028	0.145
	18.97	1.010	0.916	0.870	0.094	0.140
	15.81	0.806	0.788	0.739	0.018	0.068
	13.28	0.534	0.556	0.513	0.022	0.021
	11.38	0.281	0.311	0.267	0.030	0.014
	9.49	0.402	0.476	0.275	0.074	0.127
	9.04	0.228	0.378	0.321	0.150	0.093
	8.22	0.370	0.360	0.273	0.010	0.097
	6.96	0.111	0.119	0.065	0.007	0.046
	5.06	0.021	0.014	0.005	0.007	0.016
135°	25.30	1.071	0.987	0.980	0.084	0.091
	22.77	1.165	1.221	0.970	0.056	0.195
	21.50	1.334	1.142	0.962	0.192	0.372
	20.87	1.182	1.102	0.957	0.080	0.225
	20.24	1.114	1.066	0.952	0.048	0.162
	18.97	1.063	0.997	0.938	0.066	0.125
	15.81	0.917	1.016	0.874	0.099	0.044
	13.28	0.740	0.712	0.758	0.028	0.018
	9.49	0.240	0.351	0.355	0.111	0.115
	8.22	0.186	0.257	0.156	0.071	0.030
	6.96	0.277	0.330	0.459	0.053	0.182
	5.06	0.023	0.025	0.010	0.003	0.013
90°	25.30	1.143	1.117	1.002	0.026	0.141
	22.77	1.060	0.976	1.004	0.084	0.056
	21.82	0.717	0.963	1.004	0.246	0.287
	21.50	0.611	0.963	1.005	0.353	0.394
	20.87	0.861	0.963	1.005	0.103	0.144
	20.24	1.107	1.062	1.006	0.045	0.101
	18.97	1.146	1.242	1.009	0.096	0.137
	15.81	1.126	1.415	1.021	0.289	0.104
	13.28	1.112	1.336	1.055	0.225	0.057
	9.49	1.376	1.659	1.341	0.283	0.036
	8.22	1.124	1.113	1.208	0.011	0.084
	6.96	0.544	0.697	0.741	0.153	0.197
	5.06	0.051	0.082	0.070	0.030	0.018

attributed to joint interaction between the increase in added inertial moment of roll and the decrease in roll radiation damping around the natural roll period, as well as the decrease in added inertial moment of roll and the increase in roll radiation damping around the natural roll period.

3.5.4. Comparative analysis of roll RAOs

According to the numerical results of the motion RAOs aforementioned, for each configuration of the moonpool considered, the size of opening has significant influence on roll motion RAOs around the natural roll period. It is of interest to further compare the roll motion RAOs of the drillship with the conjoined double moonpool, separated double

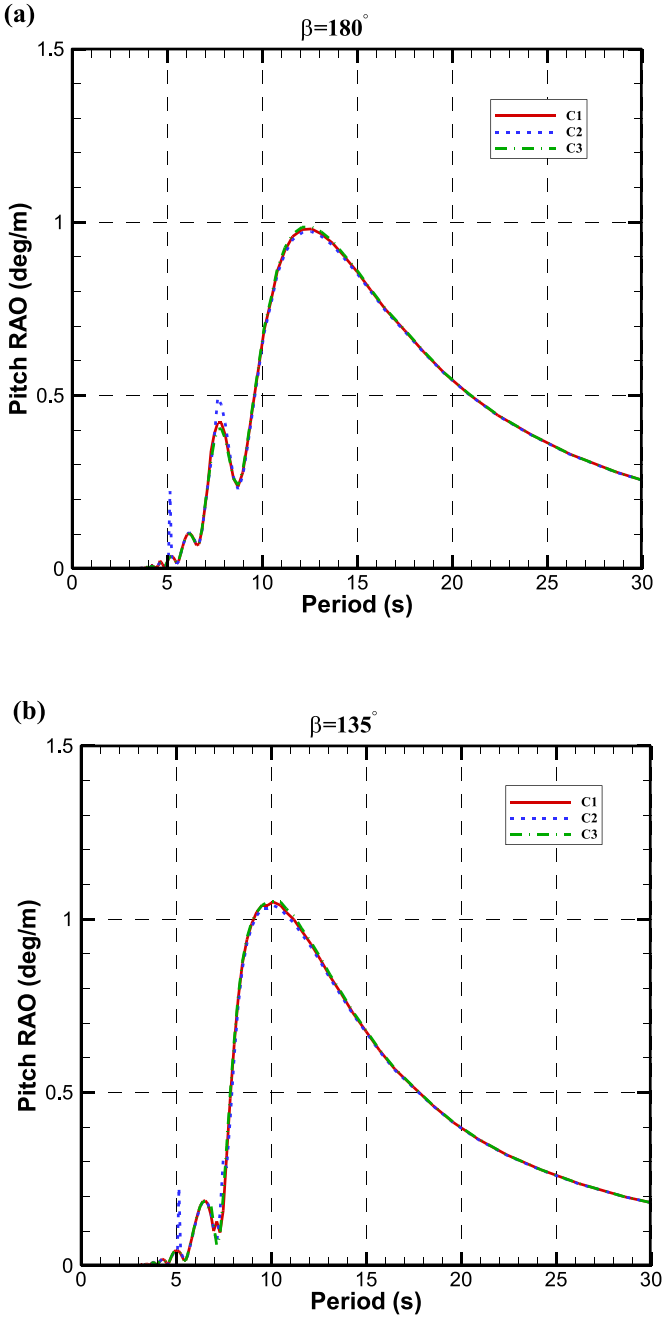

Fig. 17. Comparison of the numerical results of the pitch motion RAOs for the drillship with the single rectangular moonpool of different sizes.

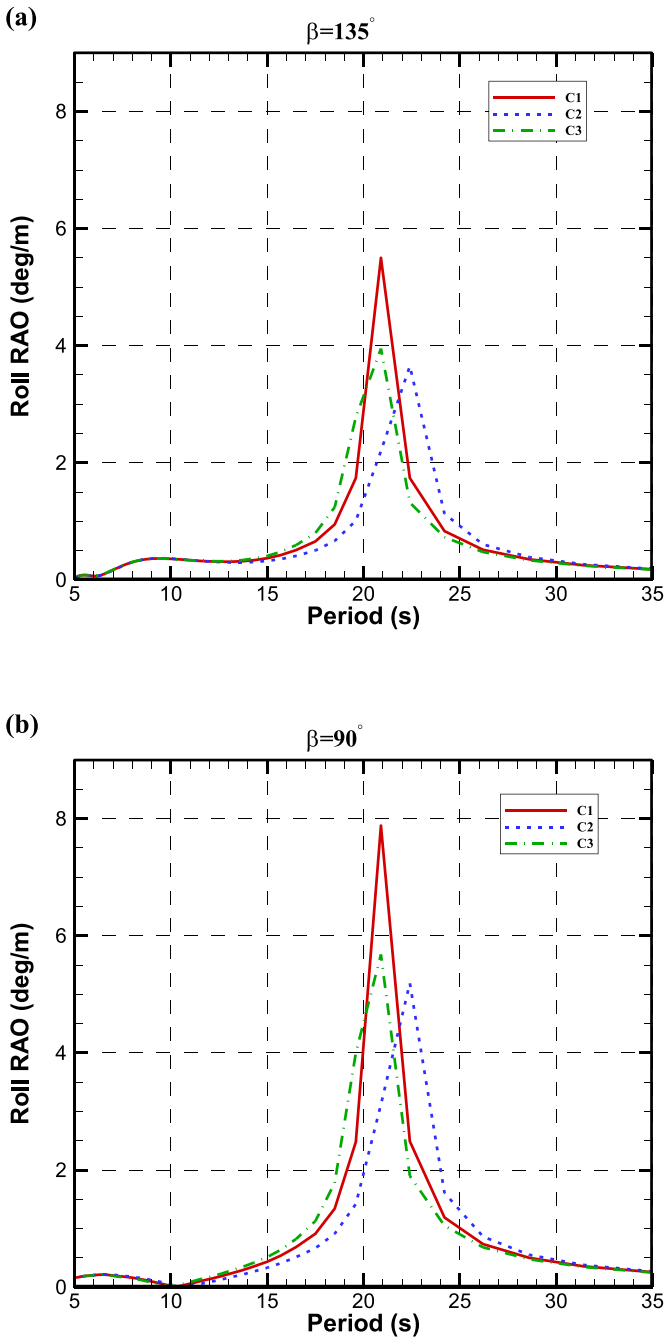

Fig. 18. Comparison of the numerical results of the roll motion RAOs for the drillship with the single rectangular moonpool of different sizes.

moonpool and single rectangular moonpool, respectively. Fig. 19 shows the roll RAO comparison of the drillship with the different moonpools in bow quartering waves. It can be seen in Fig. 19(a) that the roll RAO of the drillship with the A1 moonpool around the natural roll period is significantly less than those for the B1 and C1 moonpool, respectively. The is mainly attributed to the drillship with the A1 moonpool holds a larger draft (see in Table 2) leading to a larger added inertial moment of roll. As shown in Fig. 19(b), the roll RAO of the drillship with the C2 moonpool around the natural roll period is significantly larger than those for the A2 and B2 moonpool, respectively. This is mainly due to the larger draft for C2 induces the decrease in the roll radiation damping around the natural roll period, which dominates the roll motion compared to the increase in the added inertial moment of roll. For the drillship with the A3, B3 and C3, smaller opening leads to slight

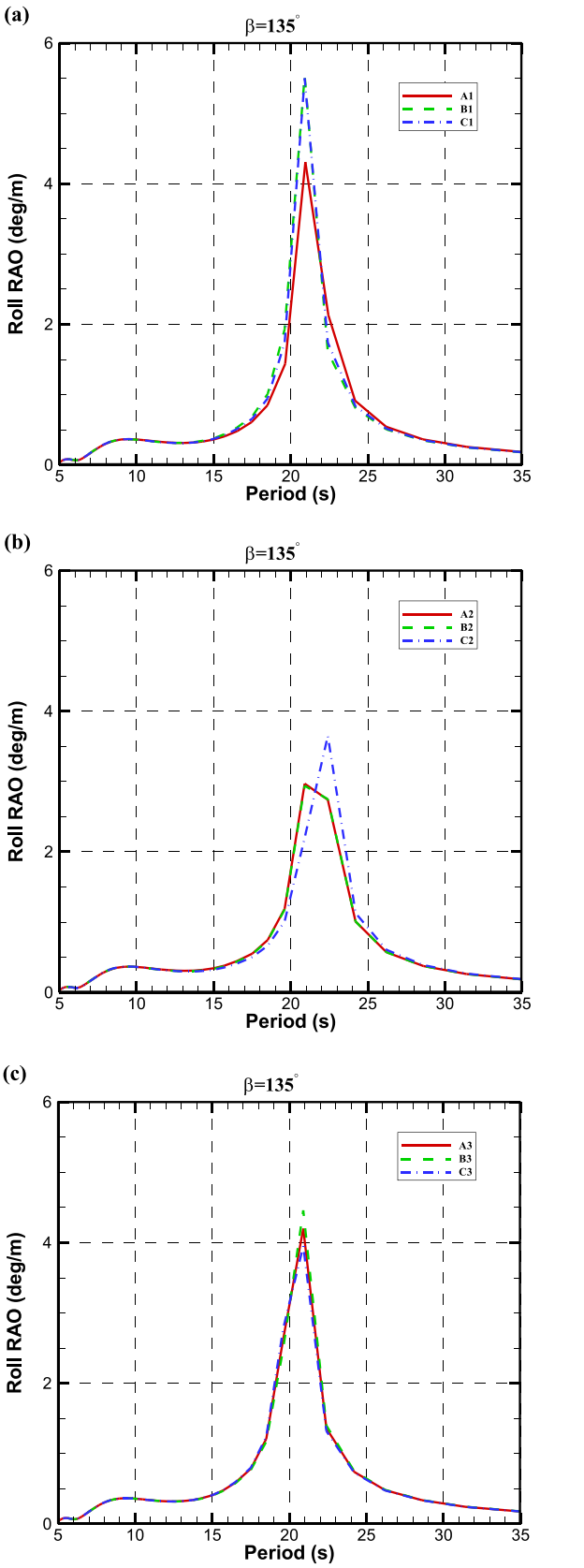

Fig. 19. Roll RAO comparison of the drillship with the different moonpools in bow quartering waves.

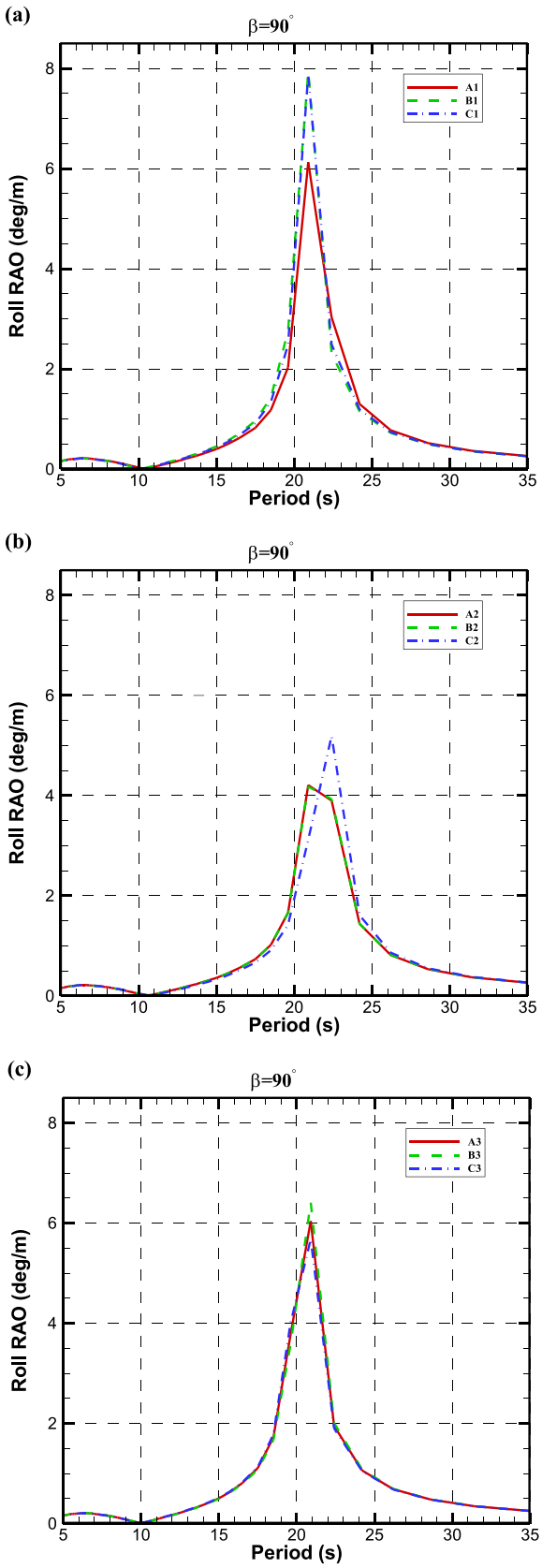

Fig. 20. Roll RAO comparison of the drillship with the different moonpools in beam waves.

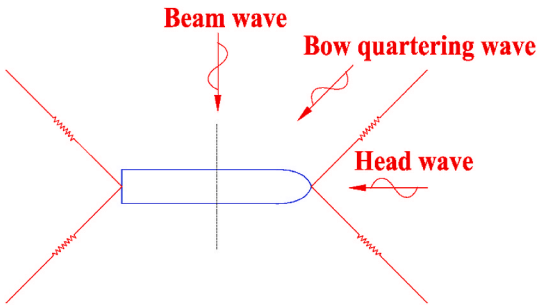

Fig. 21. Layout of the mooring system in model test.

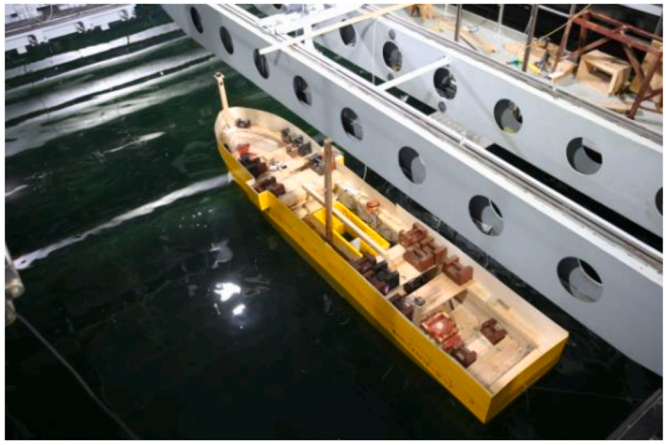

Fig. 22. Snapshot of the model in waves.

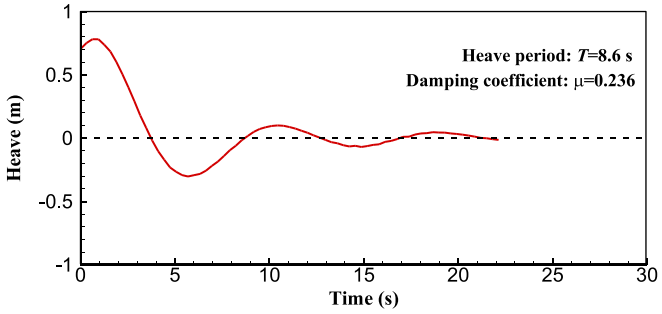

Fig. 23. Free decay curve of the heave motion.

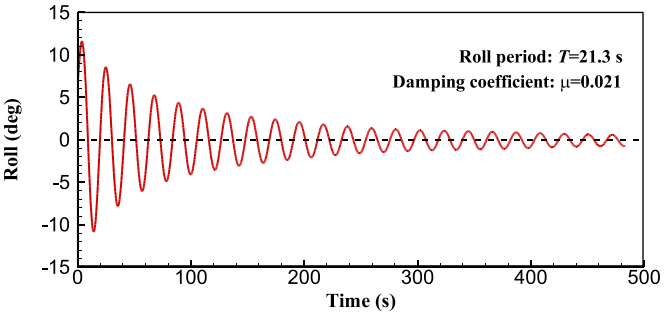

Fig. 24. Free decay curve of the roll motion.

discrepancies between the RAOs around the natural roll period as shown in Fig. 19(c). This is caused by the comparable added inertial moment of roll and roll radiation damping around the natural roll period for the

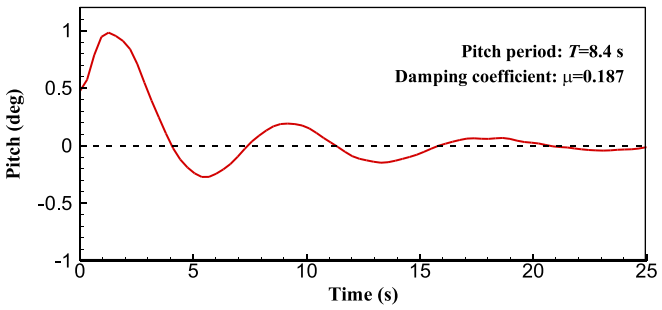

Fig. 25. Free decay curve of the pitch motion.

drillship with A3, B3 and C3, respectively. Similar but more dramatical variation tendency of the roll RAOs in beam waves can also be observed in Fig. 20, which can also be attributed to that for Fig. 19.

4. Experimental validation of motion performance

4.1. Experimental set-ups

In order to validate the numerical simulation results, a series of seakeeping model tests for the drillship with the conjoined double moonpool of the reference size (A1) were carried out in a large towing tank of Marine Design and Research Institute of China (MARIC) (Liu et al., 2020). The length of the tank is 280 m, the width is 10 m, and the water depth is 5 m. One end of the tank is a wavemaker, which can generate regular waves and irregular waves. The other end is a slope-type wave absorption beach, which is used to eliminate wave reflection. The scale ratio of the tested model is 1:40, which meets the requirement of geometric similarity. The drillship was adjusted on a trimming table to ensure the correct properties, including the mass, the centre of gravity and the radius of gyration.

In order to properly constrain the slow drift of the ship model without affecting the wave frequency motions, two steel cables connected with springs are arranged at the bow and stern of the ship model, respectively. The intersection angle between the two steel cables is 90°. The selection of the stiffness of the springs needs to ensure that the natural periods of the surge and sway motion of the moored ship model are far away from the primary wave periods during the model tests. The head wave (180°), bow quartering wave (135°) and beam wave (90°) are considered in the test. The free decay tests in still water were conducted to obtain the natural period in heave, roll and pitch mode as well as damping coefficient. Following the above tests, both regular waves and white noise irregular waves were carried out. The wave height and significant wave height of the regular waves and white noise irregular waves used in the experiments are 5 cm and 6 cm in model scale, respectively. For each white noise test, the time duration is about 10 min in model scale corresponding to 1 h in prototype. Fig. 21 shows the layout of the mooring system for the model test. Fig. 22 shows a snapshot of the model in waves.

A non-contact optical 6-DOF motion measuring instrument is used to measure the 6-DOF motions of the ship model in waves. The heave acceleration at the centre of gravity (COG) can be obtained by quadratic differentiation of the heave motion at the COG. The sampling frequency of model test is 20 Hz.

4.2. Free decay tests in still water

Fig. 23–25 show the free decay curves of the heave, roll and pitch motion of the ship in still water, respectively. The non-dimensional damping coefficient μ can be calculated as

$$\mu = \frac{1}{\pi}\ln\left|\frac{\phi_{An}}{\phi_{A(n+1)}}\right|,$$

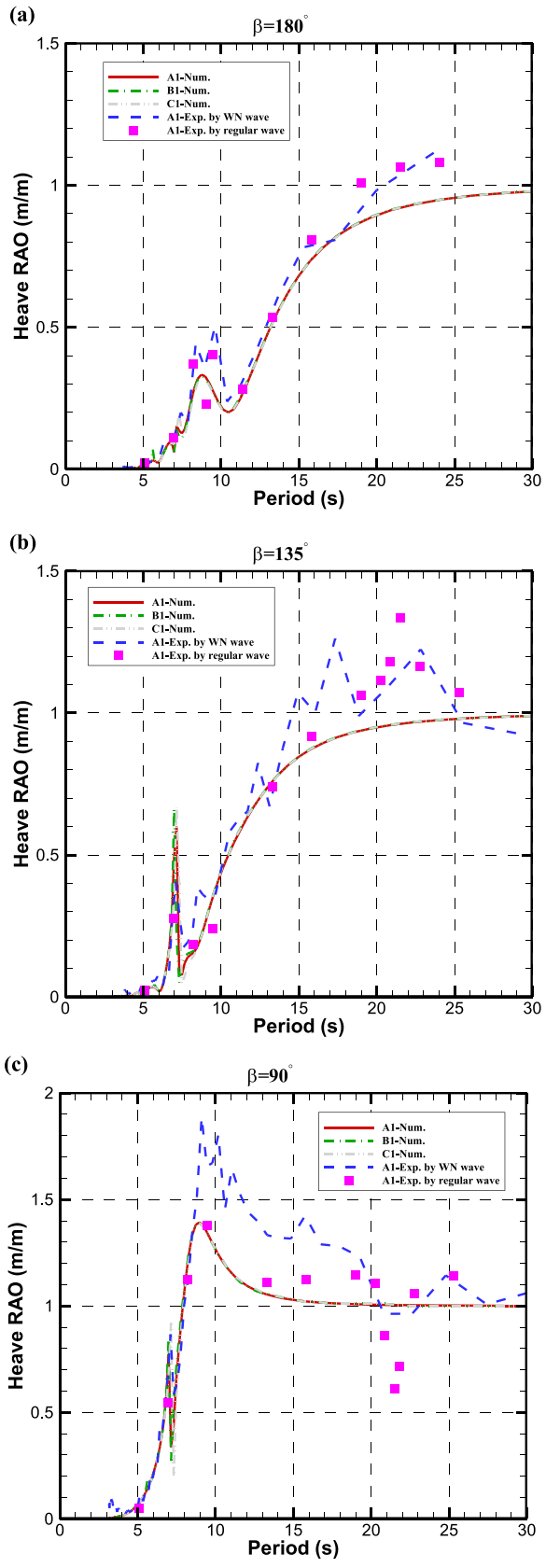

Fig. 26. Comparison of the numerical and experimental results of the heave motion RAOs for the drillship.

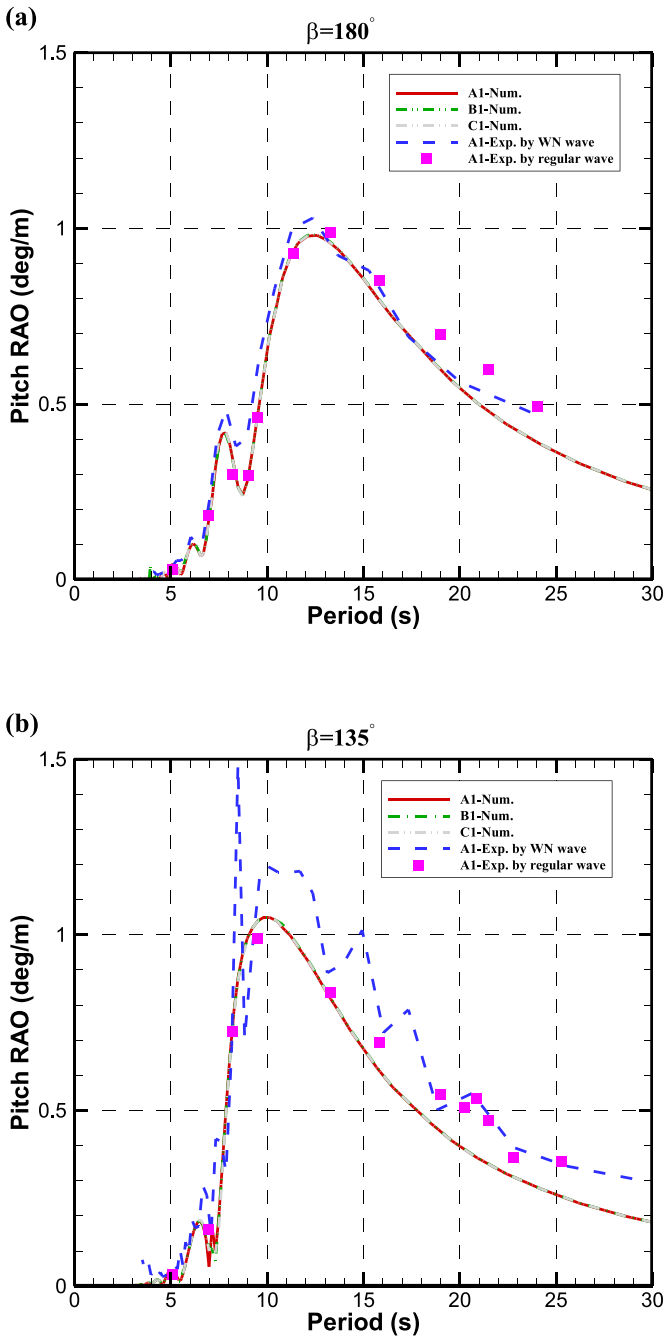

Fig. 27. Comparison of the numerical and experimental results of the pitch motion RAOs for the drillship.

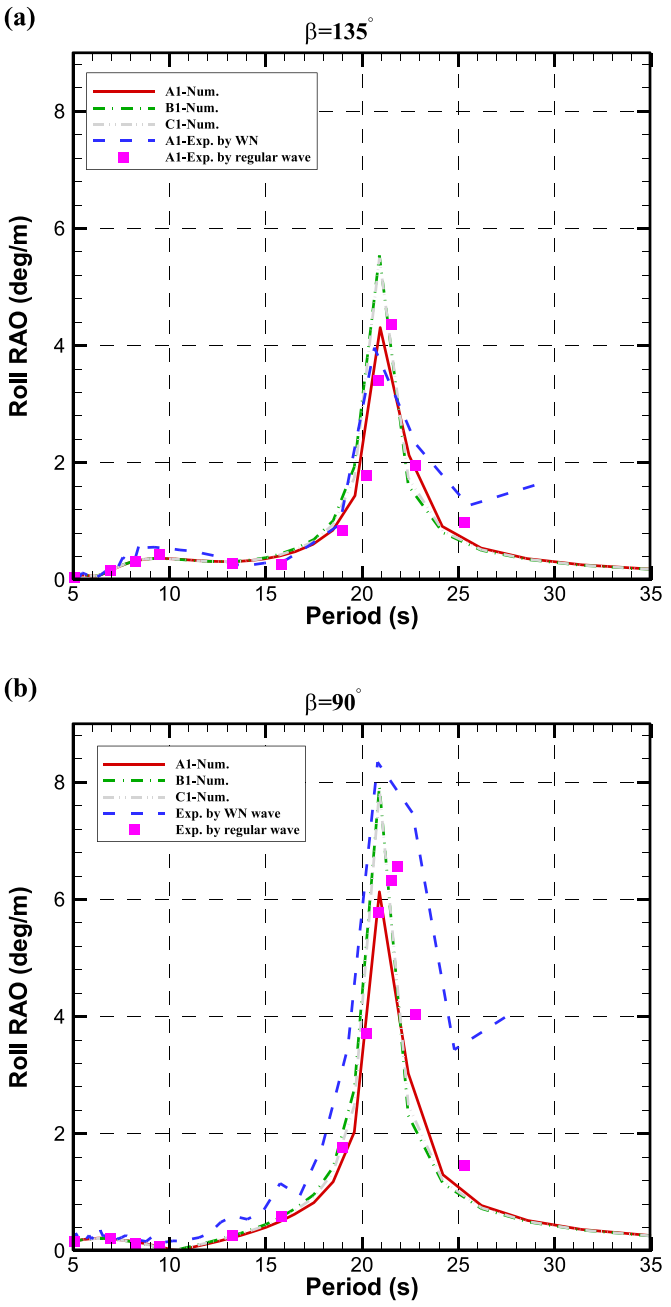

Fig. 28. Comparison of the numerical and experimental results of the roll motion RAOs for the drillship.

where $\phi_{An} > \phi_{A(n+1)}$, ϕ_{An} and $\phi_{A(n+1)}$ represent the nth and $(n+1)$th peak values or trough values of decay curves, respectively. It can be seen that the natural periods in heave, roll and pitch mode obtained in the tests agree well with those captured by the motion RAOs peaks based on numerical simulations.

4.3. Motion RAOs comparison

Fig. 26 shows the comparison of the numerical results of the heave motion RAOs of the drillship with the three types of moonpool shape of the reference size and the experimental results of the drillship with the conjoined double moonpool of the reference size. As can be seen in Fig. 26, the variation of moonpool shape has relatively prominent influence on the numerically obtained heave motion RAOs near the piston mode resonance period of the moonpool. The notable discrepancy between the numerical results and experimental results for the heave RAOs around the piston mode resonance period is due to that the present calculation method is based on linear potential theory which would over-predict the RAOs around the piston mode resonance period as pointed out by Kristiansen and Faltinsen (2008). Moreover, it can be seen that the experimental results based on regular waves as well as white noise (WN) irregular waves appear to agree well with the numerical results. It is noted that the numerical results of the heave motion RAOs near the natural roll period under the condition of bow quartering and beam waves have relatively remarkable discrepancy with the experimental results. The experimental results of the heave RAOs around the natural roll period in beam waves and bow quartering waves appears to diminish and enlarge, respectively. The decrement and increment of the heave RAOs at the natural roll period in beam waves

Table 7
Pitch RAOs deviation between the experimental results and numerical results.

Wave heading	Period (s)	Exp. of pitch RAO of A1 (deg/m)		Num. of pitch RAO of A1 (deg/m)	Absolute value of deviation (deg/m)	
		Regular waves	WN waves		regular waves & WN waves	Exp. (regular waves) & Num.
180°	24.03	0.494	0.477	0.390	0.017	0.104
	21.50	0.597	0.528	0.479	0.069	0.118
	18.97	0.698	0.612	0.599	0.085	0.098
	15.81	0.852	0.831	0.796	0.020	0.055
	13.28	0.989	0.955	0.958	0.034	0.031
	11.38	0.930	1.002	0.937	0.073	0.007
	9.49	0.461	0.598	0.462	0.137	0.002
	9.04	0.296	0.438	0.303	0.143	0.008
	8.22	0.300	0.410	0.339	0.110	0.039
	6.96	0.184	0.212	0.168	0.028	0.016
	5.06	0.030	0.038	0.042	0.008	0.012
135°	25.30	0.354	0.346	0.254	0.007	0.099
	22.77	0.367	0.398	0.311	0.032	0.055
	21.50	0.471	0.488	0.347	0.017	0.124
	20.87	0.535	0.533	0.366	0.002	0.169
	20.24	0.508	0.539	0.389	0.031	0.118
	18.97	0.546	0.506	0.441	0.040	0.105
	15.81	0.693	0.782	0.613	0.090	0.079
	13.28	0.835	0.897	0.819	0.063	0.016
	9.49	0.991	1.100	1.038	0.110	0.047
	8.22	0.724	0.839	0.752	0.116	0.029
	6.96	0.161	0.211	0.067	0.051	0.094
	5.06	0.033	0.053	0.042	0.020	0.010

Table 8
Roll RAOs deviation between the experimental results and numerical results.

Wave heading	Period (s)	Exp. of roll RAO of A1 (deg/m)		Num. of roll RAO of A1 (deg/m)	Absolute value of deviation (deg/m)	
		Regular waves	WN waves		regular waves & WN waves	Exp. (regular waves) & Num.
135°	25.30	0.985	1.355	0.706	0.371	0.279
	22.77	1.957	2.348	1.897	0.392	0.059
	21.50	4.363	3.310	3.493	1.053	0.870
	20.87	3.397	3.790	4.148	0.393	0.751
	20.24	1.788	3.289	2.761	1.502	0.974
	18.97	0.845	1.170	1.100	0.326	0.255
	15.81	0.271	0.328	0.416	0.058	0.146
	13.28	0.280	0.271	0.315	0.009	0.035
	9.49	0.440	0.550	0.367	0.110	0.073
	8.22	0.316	0.361	0.321	0.045	0.005
	6.96	0.158	0.159	0.161	0.002	0.004
	5.06	0.047	0.057	0.046	0.010	0.001
90°	25.30	1.465	3.542	1.012	2.078	0.453
	22.77	4.043	7.207	2.676	3.164	1.367
	21.82	6.560	7.861	4.229	1.302	2.330
	21.50	6.322	8.013	4.883	1.691	1.439
	20.87	5.777	8.316	6.039	2.540	0.262
	20.24	3.712	6.552	4.044	2.840	0.332
	18.97	1.767	3.104	1.546	1.337	0.221
	15.81	0.594	1.140	0.513	0.546	0.081
	13.28	0.261	0.589	0.228	0.328	0.033
	9.49	0.068	0.167	0.070	0.099	0.002
	8.22	0.132	0.165	0.156	0.033	0.024
	6.96	0.206	0.295	0.207	0.089	0.001
	5.06	0.160	0.184	0.164	0.024	0.004

and bow quartering waves are approximately 40% and 17% respectively compared to corresponding adjacent values. Such trends can also be observed in Guo et al. (2016) though less obvious compared to that in our study due to their experimental results are obtained based on white noise irregular wave tests. The energy around this frequency is not intense enough. However, the significantly more pronounced phenomenon in our study is found based on experimental measurements by regular waves which have sufficient energy to sustain this phenomenon. The enlarged heave RAOs around the natural roll period in bow quartering waves as shown in Fig. 26(b) may be due to nonlinear coupling effect in roll, pitch and heave motions. The heave RAO around the natural roll period in beam waves decreases in our study as shown in Fig. 26(c) probably due to the heave added mass or radiation damping of the drillship in beam waves is seen increases when the drillship undergoes large amplitude resonant rolling motion under the existence of a moonpool. Moreover, the effect of heave on roll RAO around the natural roll period is less probably due to the significant resonant rolling motion as pointed out by Kim et al. (2019) for a rectangular structure.

Fig. 27 shows the comparison of the numerical results of the pitch motion RAOs of the drillship with the three types of moonpool shape of the reference size and the experimental results of the drillship with the conjoined double moonpool of the reference size. It can be seen that the variation of the moonpool shape has slight influence on the pitch motion RAO, and the numerical results are in good agreement with the experimental results. Besides, the pitch RAO around the natural roll period in bow quartering waves in Fig. 27(b) can also be seen with a small enlarged tendency, probably due to coupling effect in roll, pitch and heave motions. Similar tendency can also be observed in Guo et al. (2016).

Fig. 28 shows the comparison of the numerical results of the roll motion RAOs of the drillship with the three types of moonpool shape of the reference size and the experimental results of the drillship with the conjoined double moonpool of the reference size. As can be seen in Fig. 28(a) and (b), the peak value of the roll motion RAO of the drillship with the conjoined double moonpool is approximately 30% smaller than that of the drillship with the separated double moonpool and the single rectangular moonpool of the reference size, respectively. The reason has been pointed out in the aforementioned analysis, namely the drillship with the A1 moonpool holding a dominant larger added inertial moment of roll around the natura roll period. Moreover, the numerical results of the roll motion RAO of the drillship with the conjoined double moonpool are in good agreement with the corresponding experimental results especially based on regular waves. The relatively notable discrepancy between the roll RAOs around the natural roll period based on regular waves and WN waves may be due to the error induced by calculating the ratio between a larger value of roll amplitude and a smaller value of wave amplitude when postprocessing the WN irregular waves based experimental measurements with the test duration of 10 min. This discrepancy may be reduced by a longer duration of the WN irregular waves model test.

To clearly see the discrepancy between the experimental results and numerical results, Tables 6-8 further show the heave, pitch and roll RAOs and the absolute value of the deviation between the experimental results and numerical results of the drillship with the A1 moonpool, respectively. It can be clearly seen in Tables 6-8 that the agreement between the experimental results based on regular waves and the numerical results is satisfactory except some notable discrepancies probably resulting from coupling effect aforementioned.

5. Conclusions

In this study, the influence of shape and size of the moonpool of a drillship on motion performance and static stability curve of the drillship is investigated by numerical simulation and model tests. The conclusions are drawn as follows:

(1) There is a critical heeling angle for the static stability curve of the drillship. When the heeling angle is less than the critical heeling angle, the larger the opening size of the moonpool, the larger the GZ. When the heeling angle is larger than the critical heeling angle, the larger the opening size of moonpool, the smaller the GZ.

(2) It is found that the variation of opening size of the moonpool merely has significant effect on the heave motion RAOs of the drillship near the piston resonance period of the moonpool. The larger the opening size, the larger the heave RAO around the piston resonance period. The variation of opening size of the moonpool has slight effect on the pitch motion RAOs.
(3) It is demonstrated that smaller or larger opening of the moonpool can reduce the roll motion RAO around the natural roll period of the drillship in bow quartering waves and beam waves under the condition of the same displacement. The roll motion performance of the drillship with the conjoined double moonpool of the reference size is better than that of the drillship with the separated double moonpool and the single rectangular moonpool of the reference size.
(4) It is observed in the experimental results that there exist coupling effect of roll and heave leading to the heave RAOs decreasing around the natural roll period in beam waves, as well as coupling effect in heave, pitch and roll motion RAOs around the natural roll period in bow quartering waves.

The influence of different shape and size of the moonpool on the water motion resonance inside the moonpool is not investigated in depth in this study and will be considered in future.

CRediT authorship contribution statement

Zhen Liu: lead investigator who has carried out the main investigation including numerical simulation, model testing, Formal analysis, and manuscript writing. **Jinhui He:** Researcher contributes to model tests and numerical simulation. **Yang Meng:** Researcher contributes to numerical simulation. **Haibin Zhang:** Researcher contributes to model tests. **Yaohua Zhou:** Researcher contributes to numerical simulation. **Longbin Tao:** Research collaborator contributes to project supervision, Formal analysis, and manuscript writing and revision.

Declaration of competing interest

The authors declare that they have no known competing financial interests or personal relationships that could have appeared to influence the work reported in this paper.

Data availability

Data will be made available on request.

Acknowledgements

This paper is based on the High Technology Ship Research Project. The authors would like to thank the financial support.

References

Chen, Z., Cai, S., Ye, J., Lin, X., 2018. Hydrodynamic performance analysis of drillship with different moonpool openings. China Water Trans. 18, 166–168.
Faltinsen, O.M., 1993. Sea Loads on Ships and Offshore. Cambridge University Press https://doi.org/9780521458702.
Fredriksen, A.G., Kristiansen, T., Faltinsen, O.M., 2015. Wave-induced response of a floating two-dimensional body with a moonpool. Phil. Trans. Ser. A Math. Phys. Eng. Sci. 373 https://doi.org/10.1098/RSTA.2014.0109, 2033.
Fukuda, K., 1977. Behavior of water in vertical well with bottom opening of ship, and its effects on ship-motion. J. Soc. Nav. Archit. Jpn. 107–122. https://doi.org/10.2534/jjasnaoe1968.1977.107, 1977.
Guo, X., Lu, H., Yang, J., Peng, T., 2016. Study on hydrodynamic performances of a deepwater drillship and water motions inside its rectangular moonpool. In: Proceedings of the International Offshore and Polar Engineering Conference, pp. 112–118.
Han, J., Zhang, X., Yeung, R.W., 2022. Hydrodynamic behavior of a circular floating solar pond with an entrapped two-layer fluid. Phys. Fluids 34, 012114. https://doi.org/10.1063/5.0075773.
Kawabe, H., Kwak, H.U., Park, J.J., Ha, M.K., 2010. The numerical and experimental study on moonpool water surface response of a ship in wave condition. In: Proceedings of the International Offshore and Polar Engineering Conference.
Kim, M., Jung, K.H., Park, S., Suh, S.B., Park, I.R., Kim, J., Kim, K.S., 2019. Experimental study on viscous effect in roll and heave motions of a rectangular structure. Ocean Eng. 171, 250–258. https://doi.org/10.1016/J.OCEANENG.2018.11.004.
Kristiansen, T., Faltinsen, O.M., 2008. Application of a vortex tracking method to the piston-like behaviour in a semi-entrained vertical gap. Appl. Ocean Res. 30, 1–16. https://doi.org/10.1016/J.APOR.2008.02.003.
Liu, X., Zhang, H., 2013. Analysis of motion performance for a deepwater drillship. Ship & Boat 24, 12–15.
Liu, Z., Fan, S., Wang, H., Chen, X., 2020. Study on sea-keeping model test based on transient Gaussian wave packets. Shipbuilding of China 61, 43–51.
Mavrakos, S.A., 1988. Hydrodynamic coefficients for a thick-walled bottomless cylindrical body floating in water of finite depth. Ocean Eng. 15, 213–229. https://doi.org/10.1016/0029-8018(88)90040-6.
Molin, B., 2017. On natural modes in moonpools with recesses. Appl. Ocean Res. 67, 1–8. https://doi.org/10.1016/j.apor.2017.05.010.
Molin, B., 2001. On the piston and sloshing modes in moonpools. J. Fluid Mech. 430, 27–50. https://doi.org/10.1017/S0022112000002871.
Molin, B., Zhang, X., Huang, H., Remy, F., 2018. On natural modes in moonpools and gaps in finite depth. J. Fluid Mech. 840, 530–554. https://doi.org/10.1017/JFM.2018.69.
Newman, J.N., 2018. Resonant response of a moonpool with a recess. Appl. Ocean Res. 76, 98–109. https://doi.org/10.1016/J.APOR.2018.04.016.
Sheng, Z., Yang, S., Chen, X., 1992. Ship Hydrostatics. Shanghai Jiao Tong University Press.
Sivabalan, P., Surendran, S., 2017. Numerical and experimental study on varying cross-section of moonpool for a drill ship. Ships Offshore Struct. 12, 885–892. https://doi.org/10.1080/17445302.2017.1301340.
Song, W., Li, X., Tong, B., 2018. Influence of moon pool opening on hydrodynamic performance of drillship in wave conditions. Ship Eng 40, 15–20. https://doi.org/10.13788/j.cnki.cbgc.2018.03.015.
M.Sc. thesis Sun, C., 2013. Research on Hydrodynamic Performance of a Deepwater Drillship. Shanghai Jiao Tong University.
Wei, Y., Yang, J., Chen, G., Hu, Z., 2011. The research of moonpool size effect on the hydrodynamic performance of FDPSO. In: Proceedings of the International Conference on Offshore Mechanics and Arctic Engineering - OMAE, pp. 459–467. https://doi.org/10.1115/OMAE2011-49586.
Xianyu, C., Lv, H., 2018. Hydrodynamic performance of the fluid inside the vessel moonpool in wave conditions. Ship Sci. and Tech. 40, 62–69.
Yeung, R.W., Seah, R.K.M., 2007. On Helmholtz and higher-order resonance of twin floating bodies. J. Eng. Math. 58 (1 58), 251–265. https://doi.org/10.1007/S10665-006-9109-3, 2007.
Zhang, L., Yang, Z., Zhao, Z., Cao, K., 2018. Effect of moon pool resonance on motion performance of ultra-deepwater drillship. Ship Eng 40, 14–18. https://doi.org/10.13788/j.cnki.cbgc.2018.05.014.
Zhang, X., Hu, K., Zhou, W., 2016. Motion Performance of drillship with moonpool. Ship & Boat 27, 29–36. https://doi.org/10.19423/j.cnki.31-1561/u.2016.01.004.